

Pronociceptive and Antinociceptive Effects of Buprenorphine in the Spinal Cord Dorsal Horn Cover a Dose Range of Four Orders of Magnitude

Katharina J. Gerhold,*  Ruth Drdla-Schutting,* Silke D. Honsek, Liesbeth Forsthuber, and  Jürgen Sandkühler

Department of Neurophysiology, Center for Brain Research, Medical University of Vienna, 1090 Vienna, Austria

Due to its distinct pharmacological profile and lower incidence of adverse events compared with other opioids, buprenorphine is considered a safe option for pain and substitution therapy. However, despite its wide clinical use, little is known about the synaptic effects of buprenorphine in nociceptive pathways. Here, we demonstrate dose-dependent, bimodal effects of buprenorphine on transmission at C-fiber synapses in rat spinal cord dorsal horn *in vivo*. At an analgesically active dose of $1500 \mu\text{g}\cdot\text{kg}^{-1}$, buprenorphine reduced the strength of spinal C-fiber synapses. This depression required activation of spinal opioid receptors, putatively μ_1 -opioid receptors, as indicated by its sensitivity to spinal naloxone and to the selective μ_1 -opioid receptor antagonist naloxonazine. In contrast, a 15,000-fold lower dose of buprenorphine ($0.1 \mu\text{g}\cdot\text{kg}^{-1}$), which caused thermal and mechanical hyperalgesia in behaving animals, induced an enhancement of transmission at spinal C-fiber synapses. The ultra-low-dose buprenorphine-induced synaptic facilitation was mediated by supraspinal naloxonazine-insensitive, but CTOP-sensitive μ -opioid receptors, descending serotonergic pathways, and activation of spinal glial cells. Selective inhibition of spinal 5-hydroxytryptamine-2 receptors (5-HT₂Rs), putatively located on spinal astrocytes, abolished both the induction of synaptic facilitation and the hyperalgesia elicited by ultra-low-dose buprenorphine. Our study revealed that buprenorphine mediates its modulatory effects on transmission at spinal C-fiber synapses by dose dependently acting on distinct μ -opioid receptor subtypes located at different levels of the neuraxis.

Key words: buprenorphine; descending facilitation; opioid; pain; spinal cord; synapse

Introduction

Opioids are widely used in pain therapy. Clinically used opioids mainly bind to μ -opioid receptors, which are expressed throughout the nervous system (Pert and Snyder, 1973). Despite a lack of genetic proof, pharmacology suggests that μ -opioid receptors might be divided into subtypes that can be distinguished by the μ_1 -opioid receptor subtype antagonist naloxonazine (Wolozin and Pasternak, 1981; Pasternak and Pan, 2013). A major part of opioid-induced analgesia depends on a strong, reversible depression of synaptic strength at C-fibers terminating in the superficial spinal dorsal horn (Kohnno et al., 1999; Drdla et al., 2009; Heinke et al., 2011).

The use of opioids is often limited by the development of side effects such as opioid-induced hyperalgesia (OIH), which is char-

acterized by paradoxically increased pain sensitivity involving both peripheral and central mechanisms (Colpaert, 1979; Mao et al., 1995; Célèrier et al., 1999). OIH can be observed during acute or sustained opioid treatment and upon withdrawal in humans and animals (Angst and Clark, 2006; Lee et al., 2011). At the spinal level, opioid withdrawal induces LTP at C-fiber synapses (Drdla et al., 2009; Heintz et al., 2011), which might contribute to the mechanical and thermal OIH that is induced upon withdrawal from opioids such as remifentanyl, fentanyl, and morphine (Heintz et al., 2011). However, the role of opioid receptor activation in the development of OIH has been controversial (Simonnet and Rivat, 2003; Gardell et al., 2006; Juni et al., 2007; Waxman et al., 2009; Xu et al., 2014). Recent data suggest that nonopioid receptors, such as toll-like receptor 4 (TLR4), might also be involved (Hutchinson et al., 2007; Eidson and Murphy, 2013; but see Fukagawa et al., 2013; Mattioli et al., 2014).

Another mechanism contributing to OIH is descending facilitation originating from the rostral ventromedial medulla (Vanderah et al., 2001a; Ossipov et al., 2004). Opioids may activate descending, serotonergic pathways acting on spinal 5-hydroxytryptamine-3 receptor (5-HT₃R), thereby facilitating spinal synaptic transmission (Suzuki et al., 2004; Heintz et al., 2011).

The opioid buprenorphine was synthesized in an attempt to create an opioid lacking most of the undesirable side effects but retaining an analgesic potency of morphine (Campbell and Lovell, 2012). Buprenorphine is considered to be an extraordi-

Received Feb. 21, 2014; revised May 4, 2015; accepted May 10, 2015.

Author contributions: K.J.G., R.D.-S., and J.S. designed research; K.J.G., R.D.-S., S.D.H., and L.F. performed research; K.J.G. and R.D.-S. analyzed data; K.J.G., R.D.-S., and J.S. wrote the paper.

This work was supported by the Austrian Science Fund (Grant P22306-B19 to J.S.).

The authors declare no competing financial interests.

*K.J.G. and R.D.-S. contributed equally to this work.

This article is freely available online through the JNeurosci Author Open Choice option.

Correspondence should be addressed to Jürgen Sandkühler, MD, PhD, Department of Neurophysiology, Center for Brain Research, Medical University of Vienna, Spitalgasse 4, A-1090 Vienna, Austria. E-mail: juergen.sandkuehler@meduniwien.ac.at.

DOI:10.1523/JNEUROSCI.0731-14.2015

Copyright © 2015 Gerhold, Drdla-Schutting et al.

This is an Open Access article distributed under the terms of the Creative Commons Attribution License Creative Commons Attribution 4.0 International, which permits unrestricted use, distribution and reproduction in any medium provided that the original work is properly attributed.

nary safe opioid with regard to side effects and toxicity and is therefore widely used in pain and substitution therapy. Despite this widespread use, buprenorphine's mechanisms of action are only marginally understood and its effects on synaptic transmission in the dorsal horn are virtually unknown. Recently, investigators who specifically screened for drug effects at ultra-low, subanalgesic doses reported that buprenorphine may induce hyperalgesia (Wala and Holtman, 2011), but the underlying mechanisms were not examined.

Here, we show that buprenorphine exerts dose-dependent, bimodal effects on synaptic strength at spinal C-fibers. At analgesic doses, buprenorphine inhibited synaptic strength. In contrast, a 15,000-fold lower, subanalgesic dose facilitated synaptic strength and induced hyperalgesia in behaving animals. The pronociceptive effect required activation of spinal 5-HT₂R_s via descending serotonergic pathways and the activation of spinal glial cells.

Materials and Methods

Animals. All procedures were performed in accordance with European Communities Council directives (86/609/EEC) and were approved by the Austrian Federal Ministry of Science and Research.

To avoid potential confounding effects of hormone fluctuations in female rats, only male Sprague Dawley rats (Institute for Experimental Animal Breeding of the Medical University of Vienna, Himberg, Austria) weighing between 150 and 250 g (unless stated otherwise) were used for all experiments. Animals were provided with a standard laboratory diet and water *ad libitum* and kept on a 12 h light/dark cycle, housed three to six rats per cage.

Animal surgery for electrophysiological recordings in vivo. Isoflurane in 2/3 N₂O and 1/3 O₂ was used to induce (4 vol% inspiratory) and maintain (1.5 vol% expiratory) anesthesia. Concentrations of blood gases were measured and monitored with a capnograph (Capnomac Ultima; Datex-Ohmeda). Animals were intubated with a 14 G cannula for mechanical ventilation with a respirator (Servo Ventilator 900C; Siemens) and then ventilated at a rate of 75 strokes·min⁻¹ using a tidal volume of 4–6 ml. Body core temperature was maintained at 37°C with a feedback-controlled heating blanket (Panlab). Deep surgical level of anesthesia was verified by stable mean arterial blood pressure during noxious stimulation. Surgical procedures were performed as described previously (Ikeda et al., 2006). Briefly, the right jugular vein and carotid artery were cannulated to allow intravenous infusions and arterial blood pressure monitoring, respectively. The right femoral vein was cannulated for buprenorphine administration. During anesthesia, animals continuously received intravenous solution (58% Ringer's solution, 30% HAES, 8% glucose, and 4% sodium bicarbonate, 2 ml·h⁻¹) for stabilization of arterial blood pressure (mean 130–160 mmHg) and base excess (mean 1.5 ± 0.8 mmol·L⁻¹). The arterial catheter was flushed every 30 min with heparinized sodium solution (2.5 IU·ml⁻¹) to prevent blood agglutination. Arterial blood gas analyses were performed every 60 min. Muscle relaxation was achieved by 2 μg·kg⁻¹·h⁻¹ intravenous pancuronium bromide. The left sciatic nerve was dissected free for bipolar electrical stimulation with a silver hook electrode. The lumbar segments L4 and L5 were exposed by laminectomy. The dura mater was carefully incised and retracted. For the surgical spinalization experiment, cervical segments C6 and C7 were exposed by laminectomy to allow cervical spinal transection using thermal cautery (Fine Science Tools). Afterward, the wound was coated with a tissue soaked in cool 0.9% sterile NaCl solution to avert bleeding. Muscles and skin were sutured. Two metal clamps were used for fixation of the animal vertebral column in a stereotactic frame. An agarose pool was formed around the exposed spinal segments L4 and L5. The spinal cord segment was continuously superfused with 5 ml of artificial CSF (ACSF) containing the following (in mM): 135 NaCl, 1.7 KCl, 1.8 CaCl₂, 10 HEPES, and 1 MgCl₂, pH 7.2, 275–290 mOsm·kg⁻¹, in which additional drugs were dissolved as indicated. At the end of each experiment, animals were killed by decapitation, and the spinal cord was removed and cryofixed for detection of a rhodamine B spot at the recording site under a fluorescence microscope.

Only those experiments in which the recording site was located in laminae I or II were taken for further analysis.

Electrophysiological recordings in vivo. Electrophysiological recordings were performed as described previously (Ikeda et al., 2006). Briefly, C-fiber-evoked field potentials were recorded with glass microelectrodes (impedance of 2–3 MΩ) from laminae I and II of the spinal cord dorsal horn in response to electrical stimulation of the sciatic nerve in C-fiber strength using an electrical stimulator (ISO STIM 01 D; NPI Electronic). The pipette solution consisted of ACSF with 0.2% rhodamine B. Electrodes were driven by a microstepping motor. Recordings were made with an EXT 02/F-amplifier (NPI Electronics) using a bandwidth filter of 0.1–1000 Hz. Signals were monitored on a digital oscilloscope and digitized by an analog-to-digital converter. Test stimuli were delivered to the sciatic nerve and consisted of pulses of 0.5 ms duration at C-fiber intensity (25 V) given every 5 min. After obtaining a stable baseline, recordings were continued for at least 4 h. C-fiber-evoked potentials had a long latency (≈80 ms), corresponding to a conduction velocity of C-fibers of <1 m/s. At the end of each electrophysiological experiment, pressure was applied to the electrode (300 mbar, 1 min) and recording sites were verified histologically with the rhodamine dye.

Calcium imaging. Male postnatal day 20 (P20)–P25 rats were deeply anesthetized and decapitated. The lumbar spinal cord was removed after a dorsal laminectomy and ≈500-μm-thick transverse spinal cord slices were cut with a vibrating microslicer (DTK-1000; Dosaka) as described previously (Heinke et al., 2011). The dissection was performed in chilled incubation solution consisting of the following (in mM): 95 NaCl, 1.8 KCl, 1.2 KH₂PO₄, 0.5 CaCl₂, 7 MgSO₄, 26 NaHCO₃, 15 glucose, and 50 sucrose, oxygenated with 95% O₂ and 5% CO₂, resulting in a pH of 7.4 and 310–320 mOsm/kg. After being kept at 34°C for 30 min, slices were allowed to rest at room temperature until use. Imaging experiments were performed at room temperature in recording solution that was identical to the incubation solution, with the following exceptions (in mM): 127 NaCl, 2.4 CaCl₂, 1.3 MgSO₄, and 0 sucrose. To image calcium, astrocytes were loaded with the fluorescent indicator Fluo-5F (F5F) via patch pipettes (3–5 MΩ resistance), as described previously (Honsek et al., 2012). In brief, patch pipettes were filled with intracellular solution consisting of the following (in mM): 120 K-MeSO₃, 20 KCl, 2 MgCl₂, 20 HEPES, 0.2 EGTA, 2 Na₂ATP, and 0.5 NaGTP, as well as 0.1 AlexaFluor 594 (AF594) and 0.4 F5F, pH 7.28 with KOH. After establishing the whole-cell configuration, electrophysiological properties were determined with an Axopatch 200B amplifier coupled to a Digidata 1440 interface (Molecular Devices). The pClamp10 software package was used. After confirming that recorded cells exhibited electrophysiological characteristics of astrocytes (low input resistance, linear current–voltage relationship, membrane potential more negative than –70 mV, and no action potentials upon depolarization in current-clamp mode), patch pipettes were carefully withdrawn and tetrodotoxin (1 μM) was applied for at least 5 min in all experiments. The 5-HT_{2A}, 5-HT_{2B}, and 5-HT_{2C} receptor (5-HT_{2A}R, 5-HT_{2B}R, 5-HT_{2C}R) antagonists 200 μM 4F 4FP, 100 μM SB 204741, and 100 nM RS 102221, respectively, were applied with the recording solution for at least 15 min as required. Calcium imaging was performed via multiphoton imaging on a Leica DM6000CFS microscope equipped with a 20× objective [Leica HCX APO, numerical aperture (NA) 1.0] and a Chameleon-XR Ti-sapphire laser (Coherent Technologies). AF594 and F5F were excited at 810 nm and fluorescence emission was collected with nondescanned detectors at 565–605 nm and 500–550 nm, respectively. Images were collected at 2 Hz and the 5-HT_{2A}R, 5-HT_{2B}R, and 5-HT_{2C}R agonists TCB-2, BW 723C86, and CP 809101 (all 5 mM) were puff applied for 200 ms via a patch pipette coupled to a picospritzer. Data were collected from AF594-filled astrocytes with cell somata within 60 μm distance of the application pipette (patched cell and 1–2 cells filled via gap junctions) and are expressed as changes in fluorescence intensity relative to baseline fluorescence (ΔF/F).

Drugs. For *in vivo* electrophysiological recordings, pancuronium bromide (Pancuronium-ratiopharm; Ratiopharm) was administered as an intravenous infusion (2 μg·kg⁻¹·h⁻¹). Buprenorphine (Bupaq; Richter Pharma) was applied as intravenous bolus injection (1500 μg·kg⁻¹ for analgesic dose experiments and 0.1 μg·kg⁻¹·h⁻¹ for ultra-low-dose experiments in a total volume of 1 ml diluted in physiological saline) into

Table 1. Response values and statistics before and after antagonist application obtained in *in vivo* electrophysiological experiments

Figure(s)	Treatment	Administration mode	Pre-antagonist vs post-antagonist values	<i>p</i> -value
2B, 3B	Naloxone hydrochloride	Intravenous	102 ± 6% vs 138 ± 16%	<0.001
2C, 3C	Naloxone methiodide	Intravenous	100 ± 4% vs 124 ± 10%	<0.001
2D, 3D	Naloxone hydrochloride	Spinal	99 ± 3% vs 113 ± 6%	<0.001
2E, 3E	CTOP	Intravenous	102 ± 5% vs 119 ± 8%	<0.001
5B	Granisetrone	Spinal	99 ± 4% vs 132 ± 15%	<0.001
5C,F	Asenapine	Spinal	99 ± 4% vs 129 ± 8%	<0.001
6A	4F 4PP	Spinal	98 ± 6% vs 140 ± 18%	<0.001
6B	SB 204741	Spinal	101 ± 4% vs 131 ± 15%	<0.001
6C	RS 102221	Spinal	102 ± 5% vs 124 ± 12%	0.002
6D	4F 4PP, SB 204741, RS 102221	Spinal	101 ± 6% vs 130 ± 10%	<0.001
9A	Fluorocitrate	Spinal	98 ± 4% vs 105 ± 14%	0.4
9C	DAAO	Spinal	100 ± 4% vs 137 ± 10%	<0.001
9D	D-AP5	Spinal	100 ± 9% vs 97 ± 6%	0.6

Values represent mean areas of C-fiber-evoked field potentials ± SEM. Data were normalized to the last five time points before antagonist application. *p*-values were obtained via paired *t* test.

Table 2. Response values and statistics of untreated and treated rats obtained in behavioral experiments

Figure	Treatment	Test	Pretreatment	Posttreatment	Treatment		Interaction		Time		<i>p</i> -values for single time points			
					<i>p</i>	<i>F</i>	<i>p</i>	<i>F</i>	<i>p</i>	<i>F</i>	–1 d	3 h	6 h	24 h
1A	Analgesic-dose bup (1500 μg·kg ^{–1})	Hargreaves (s)	4.5 ± 0.2	8.4 ± 0.4	<0.001	124.30	<0.001	22.95	<0.001	22.62	0.94 (<i>n</i> = 9)	<0.001 (<i>n</i> = 9)	<0.001 (<i>n</i> = 9)	X
1B	Ultra-low-dose bup (0.1 μg·kg ^{–1})	Hargreaves (s)	10.4 ± 0.5	8.1 ± 0.5	0.009	7.00	0.150	1.82	0.003	5.10	>0.99 (<i>n</i> = 14)	0.04 (<i>n</i> = 14)	0.01 (<i>n</i> = 14)	>0.99 (<i>n</i> = 6)
1C	Ultra-low-dose bup (0.1 μg·kg ^{–1})	Von Frey (g)	12.2 ± 0.3	6.5 ± 0.9	<0.001	15.30	0.001	5.97	<0.001	8.13	>0.99 (<i>n</i> = 14)	0.005 (<i>n</i> = 11)	<0.001 (<i>n</i> = 14)	>0.99 (<i>n</i> = 6)
4A	CTOP + ultra- low-dose bup (s)	Hargreaves (s)	9.8 ± 0.6	9.3 ± 0.5	<0.001	12.52	0.291	1.27	0.16	1.88	>0.99 (<i>n</i> = 9)	>0.99 (<i>n</i> = 9)	>0.99 (<i>n</i> = 9)	X
4B	CTOP + ultra- low-dose bup (g)	Von Frey (g)	12.4 ± 0.3	11.5 ± 0.8	<0.001	32.79	<0.001	9.42	<0.001	21.45	>0.99 (<i>n</i> = 9)	0.99 (<i>n</i> = 9)	>0.99 (<i>n</i> = 9)	X
7A	5-HT ₂ R antagonists + ultra-low- dose bup (s)	Hargreaves (s)	12.2 ± 0.8	12.1 ± 0.8	<0.001	19.70	<0.001	5.90	0.001	7.50	0.92 (<i>n</i> = 9)	0.57 (<i>n</i> = 9)	0.98 (<i>n</i> = 9)	X
7B	5-HT ₂ R antagonists + ultra-low- dose bup (g)	Von Frey (g)	12.6 ± 0.2	11.7 ± 0.5	<0.001	24.51	<0.001	6.52	<0.001	12.46	>0.99 (<i>n</i> = 9)	>0.99 (<i>n</i> = 9)	>0.99 (<i>n</i> = 9)	X

Values represent mean responses ± SEM obtained in Hargreaves or von Frey experiments. Data were analyzed using a two-way ANOVA with time and treatment as dependent variables with Bonferroni's correction. *p*- and *F*-values for "treatment" indicate the general treatment effect determined by two-way ANOVA. In addition, *p*- and *F*-values for interaction and time obtained by two-way ANOVA are stated. Single time point *p*- and *F*-values were obtained via multiple comparisons. "X" indicates absence of testing at this time point. Mean response values of vehicle-treated control animals remained unchanged compared with baseline at all time points (*p* > 0.05). bup, Buprenorphine.

the right femoral vein. In general, drugs were applied after a 30 min stable baseline recording period 60 min before buprenorphine injection. The opioid receptor antagonist naloxone hydrochloride (100 μg·kg^{–1}·h^{–1}; Tocris Bioscience) and the peripherally restricted opioid receptor antagonist naloxone methiodide (20 mg·kg^{–1}·h^{–1}; Sigma-Aldrich) were applied as a continuous intravenous infusion into the right jugular vein at indicated concentrations starting 60 min before buprenorphine injection and lasting throughout the recording period. The μ-opioid receptor antagonists D-Phe-Cys-Tyr-D-Trp-Orn-Thr-Pen-Thr-NH₂ (CTOP; 1 mg·kg^{–1}) and D-Phe-Cys-Tyr-D-Trp-Arg-Thr-Pen-Thr-NH₂ (CTAP; 1 mg·kg^{–1}), both obtained from Tocris Bioscience, were dissolved in sterile 0.9% NaCl solution and administered as a single intravenous bolus into the jugular vein 60 min before buprenorphine injection. The μ₁-opioid receptor antagonist naloxonazine dihydrochloride (10 mg·kg^{–1}) was obtained from Tocris Bioscience and dissolved in sterile 0.9% NaCl solution. Naloxonazine was either injected intraperitoneally as a single bolus injection 24 h before surgery or intravenously 60 min before buprenorphine administration. The following drugs (obtained from Tocris Bioscience) were dissolved in water and added directly to 5 ml of ACSF superfusate 60 min before buprenorphine injection to obtain desired concentrations as indicated and were superfused by means of a roller pump at the recording site throughout the experiment: naloxone hydrochloride (100 μM); naloxone methiodide (1 mM); the competitive *N*-methyl-D-aspartate receptor (NMDAR) antagonist D-(–)-2-amino-5-phosphonopentanoic acid (D-AP5; 100 μM); the serotonin, dopamine, histamine, and noradrenalin receptor antagonist asenapine maleate (5

μM); and the 5-HT₃ receptor (5-HT₃R) antagonist granisetron hydrochloride (1 mM). The 5-HT_{2A}R, 5-HT_{2B}R, and 5-HT_{2C}R antagonists 4F 4PP (200 μM), SB 204741 (100 μM), and RS 102221 (100 nM), all obtained from Tocris Bioscience, were dissolved in DMSO and diluted in ACSF to the indicated end concentrations. The 5-HT_{2A}R, 5-HT_{2B}R, and 5-HT_{2C}R agonists TCB-2, BW 723C86, and CP 809101 (Tocris Bioscience) were prepared as a 30 mM stock solution in DMSO and diluted to an end concentration of 5 mM in ACSF. The glial toxin sodium fluorocitrate (10 μM) and D-amino acid oxidase (DAAO, 1 U/mL) were purchased from Sigma-Aldrich and diluted in water.

Behavioral experiments. Behavioral experiments were performed during the light cycle. Animals were habituated to the facility for at least 2 d and handled by the experimenter during this time. For 2 d before the assessment of baseline thresholds, rats were habituated to the behavioral testing apparatus for 60 min/d. Baseline threshold testing was initiated 1 d before treatment. Buprenorphine or physiological saline (vehicle) was injected intraperitoneally under short isoflurane anesthesia. For high-dose experiments, buprenorphine (1500 μg·kg^{–1})-treated and the respective vehicle-treated control animals were intubated and mechanically ventilated until spontaneous breathing restarted. For ultra-low-dose experiments, buprenorphine (0.1 μg·kg^{–1}) or physiological saline was injected intraperitoneally under brief isoflurane anesthesia. In one experiment, CTOP (1 mg·kg^{–1}) or saline was injected intraperitoneally 60 min before ultra-low-dose buprenorphine (or saline as vehicle) injection. To study the effect of 5-HT₂R blockade on ultra-low-dose buprenorphine-induced hyperalgesia, the 5-HT_{2A}R, 5-HT_{2B}R, and

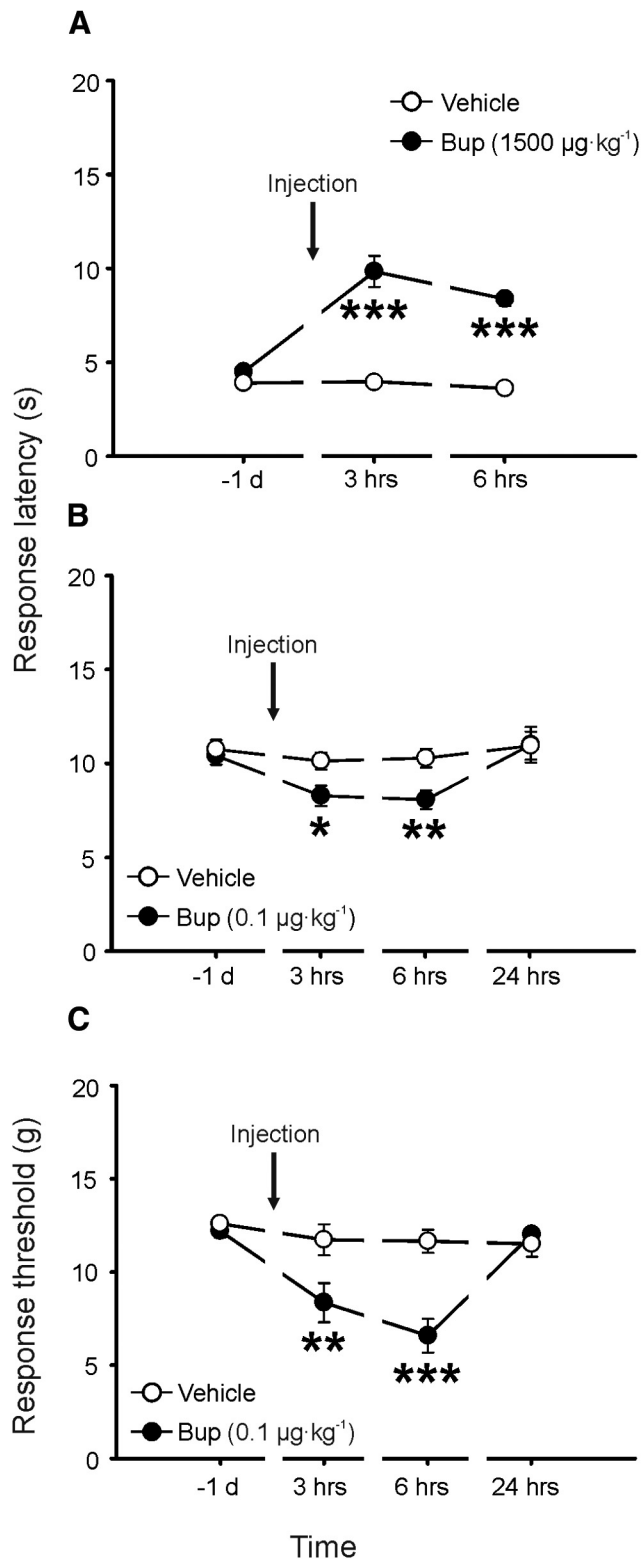


Figure 1. Ultra-low-dose buprenorphine elicits mechanical and thermal hyperalgesia, whereas a 15,000-fold higher dose of buprenorphine induces analgesia. Animals received an intraperitoneal bolus injection of buprenorphine or sterile saline as a vehicle control (black arrow) under deep anesthesia. **A, B,** Mean response latencies to radiant heat stimulation plotted at different time points. **A,** Buprenorphine at 1500 $\mu\text{g}\cdot\text{kg}^{-1}$ (black circles, $n = 9$ at all time points) enhanced mean response latencies to heat stimulation of the hindpaw compared with vehicle control (open circles, $n = 9$ at all time points). Response latencies of the control group remained stable. **B,** Ultra-low-dose buprenorphine (0.1 $\mu\text{g}\cdot\text{kg}^{-1}$, black circles, $n = 14$ at -1 d, 3 and 6 h; $n = 6$ at 24 h) reduced mean response latencies to heat stimulation of the

5-HT_{2C}R antagonists 4F 4PP (2 mM), SB 204741 (1 mM), and RS 102221 (1 μM , all in 25% DMSO/NaCl) or saline were injected intrathecally 15 min before ultra-low-dose buprenorphine injection. Transcutaneous intrathecal injections were modified from Mestre et al. (1994). Briefly, animals were anesthetized with isoflurane. The 5-HT_{2C}R antagonists were injected with a 23 G cannula connected to a 50 μl Hamilton syringe. The needle was slowly inserted between the L4 and L5 vertebrae. A quick tail flick served as control for the entrance into the intrathecal space. A total volume of 20 μl was injected.

Behavioral testing was performed at 3 and 6 h after buprenorphine injection. To determine whether ultra-low-dose buprenorphine-induced hyperalgesia was still present 24 h after injection, six animals were also tested at this late time point. Mechanical thresholds were measured with calibrated von Frey monofilaments with incremental stiffness between 0.25 and 15 g (Stoelting) based on the up and down method of Dixon (1965). Rats were placed in individual Plexiglas boxes on a wire mesh metal floor. The plantar surface of the hindpaw between the footpads was stimulated at ≈ 10 s intervals for 5 s or until a response was elicited. A foot withdrawal not attributable to normal locomotion was counted as a positive response. A lower force hair was presented after a positive response and a higher force following a negative response. A 50% threshold in grams was calculated as described previously (Chaplan et al., 1994). Experiments were performed by an experimenter unaware of treatment groups. The response latencies of both hindpaws were averaged.

For assessment of thermal thresholds, a commercially available plantar test (Ugo Basile) was used. The animals were placed on a glass floor. A short noxious stimulus was applied to the paw of the unrestrained rat (Hargreaves et al., 1988). The retraction of the paw was detected by a sensor and the latency between the onset of the heat stimulus and the reaction of the animal was noted in seconds. At each time point, three readings for each paw were performed with 15 min intervals. Because of the different heat intensities, analgesic-dose and ultra-low-dose experiments were performed separately. High-intensity radiant heat (intensity = 220 $\text{mW}\cdot\text{cm}^{-2}$, baseline = 3–4 s) was used to determine responses to analgesic doses of buprenorphine. Low-intensity radiant heat (intensity = 130 $\text{mW}\cdot\text{cm}^{-2}$, baseline = 9–11 s) was used to determine ultra-low-dose buprenorphine-induced thermal hyperalgesia.

All behavioral experiments were performed by an experimenter blinded to treatment. The response latencies of both hindpaws were averaged.

Immunohistochemistry. Thirty animals from behavioral experiments were further used for glial activation studies. After testing at 6 or 24 h after buprenorphine or vehicle injection, animals were deeply anesthetized and perfused with heparinized 0.9% saline at room temperature, followed by cold 4% paraformaldehyde and 1.5% picric acid in 0.1 M phosphate buffer. Spinal cords were removed and postfixed overnight at 4°C in the same fixative. The tissues were cryoprotected overnight in 0.1 M PB containing 20% sucrose at 4°C and then snap-frozen in isopentane (-80°C). Transverse sections of 10 μm thickness were cut from L4/L5 on a freezing microtome (Leica CM 3050S). Sections were incubated in blocking solution with 5% normal donkey serum and 0.15% Triton X-100 in PBS for 15 min. The following primary antibodies were incubated overnight at 4°C: the microglial marker ionized calcium binding adaptor molecule 1 (Iba1; goat anti-Iba1; 1:1000; Abcam ab5076), the astrocytic marker glial fibrillary acidic protein (GFAP; rabbit anti-GFAP; 1:1000; Thermo Scientific MS-1376), and the marker for neuronal nuclear antigen (NeuN; mouse anti-NeuN; 1:500; Millipore MAB 377). The secondary antibodies used were donkey anti-goat-IgG-Cy2 (1:400; Jackson Laboratories 705-225-147), donkey anti rabbit-IgG-DyLight549 (1:

hindpaw compared with vehicle control (open circles, $n = 14$ at -1 d, 3 and 6 h; $n = 6$ at 24 h). Response latencies of the control group remained stable. **C,** The mean response thresholds to probing with von Frey filaments are plotted at different time points. Ultra-low-dose buprenorphine (dosing as in **B**, black circles, $n = 14$ at -1 d and 6 h; $n = 11$ at 3 h; $n = 6$ at 24 h) reduced mean von Frey thresholds compared with vehicle control (open circles, $n = 14$ at -1 d and 6 h; $n = 11$ at 3 h; $n = 6$ at 24 h). Response thresholds of the control group remained stable. Statistics: **A–C,** Two-way ANOVA vs untreated controls (open circles) followed by Bonferroni *post hoc* test; p - and F -values are listed in Table 1 (***) $p < 0.001$, ** $p < 0.01$, * $p < 0.05$).

400; Jackson Laboratories 711-505-152) and horse anti-mouse DyLight 649 (1:400; Vector Labs DI-2649), diluted in PBS, and incubated for 2 h at room temperature.

Stained sections were observed with an Olympus BX51 fluorescent microscope and an Olympus XM10 camera was used to record images using an Olympus Plan 20 \times (NA 0.40) objective. Camera settings and exposure times were kept constant for all series of images acquired. Images were analyzed using CellD software (Olympus). For analysis of GFAP, NeuN and Iba1 immunoreactivity, images of the dorsal horn of 12 sections, which were at least 100 μ m apart, were taken. A region of interest (ROI) was drawn covering LI/II of the spinal cord dorsal horn. Borders were set at \sim 120 μ m from the dorsal white matter border. The mean pixel intensities for GFAP and Iba1 in a given ROI was measured and normalized to NeuN intensity within the same ROIs. Analysis was performed by a person blinded to the treatment.

Statistical analysis. Data were analyzed using GraphPad Prism 6 or SigmaStat 3.1 (Systat Software) software. For electrophysiological recordings, the area under the curve of C-fiber-evoked field potentials was determined offline using Clampfit 10 (Molecular Devices). The mean area under the curve of five consecutive field potentials before opioid application served as a baseline control. Responses were normalized to the baseline in every animal. Data were tested for normality using the Shapiro–Wilk test and for equal variances using Levene’s test. A two-way ANOVA followed by Bonferroni *post hoc* tests for multiple comparisons were performed (factor 1: treatment; factor 2: time) to compare different treatments and to assess the final size of potentiation or depression from treated animals at time points indicated in the text. Antagonist treatments were compared with either untreated controls or buprenorphine-treated animals without antagonist. The effects of the respective antagonists on baseline are shown in Table 1. Behavioral data were analyzed using a two-way ANOVA followed by Bonferroni *post hoc* test for multiple comparisons comparing treatments and time points. ANOVA results for factor “treatment” are given as the value of the Fisher distribution $F_{(x,y)}$ obtained from the data, where x is the degrees of freedom for groups and y is the total degrees of freedom of the distribution. For immunohistochemistry data, a t test was performed to compare normalized GFAP and Iba1 intensities of buprenorphine- and vehicle-treated animals. For calcium-imaging experiments, a Mann–Whitney rank-sum test was used for group analysis of the amplitudes because the Shapiro–Wilk normality test failed. The number of responding astrocytes was analyzed with a z test.

The numerical value of p given in the figure legends is the value of the variance analysis. p -values in text represent values of *post hoc* tests, unless stated otherwise. A p -value of < 0.001 was considered as statistically “highly significant” and a p -value < 0.05 as “significant.” Values are expressed as mean \pm SEM. Note that, in Figures 2C, 3D, 5B, E, F, 6A–C, and 9A, although there are overall

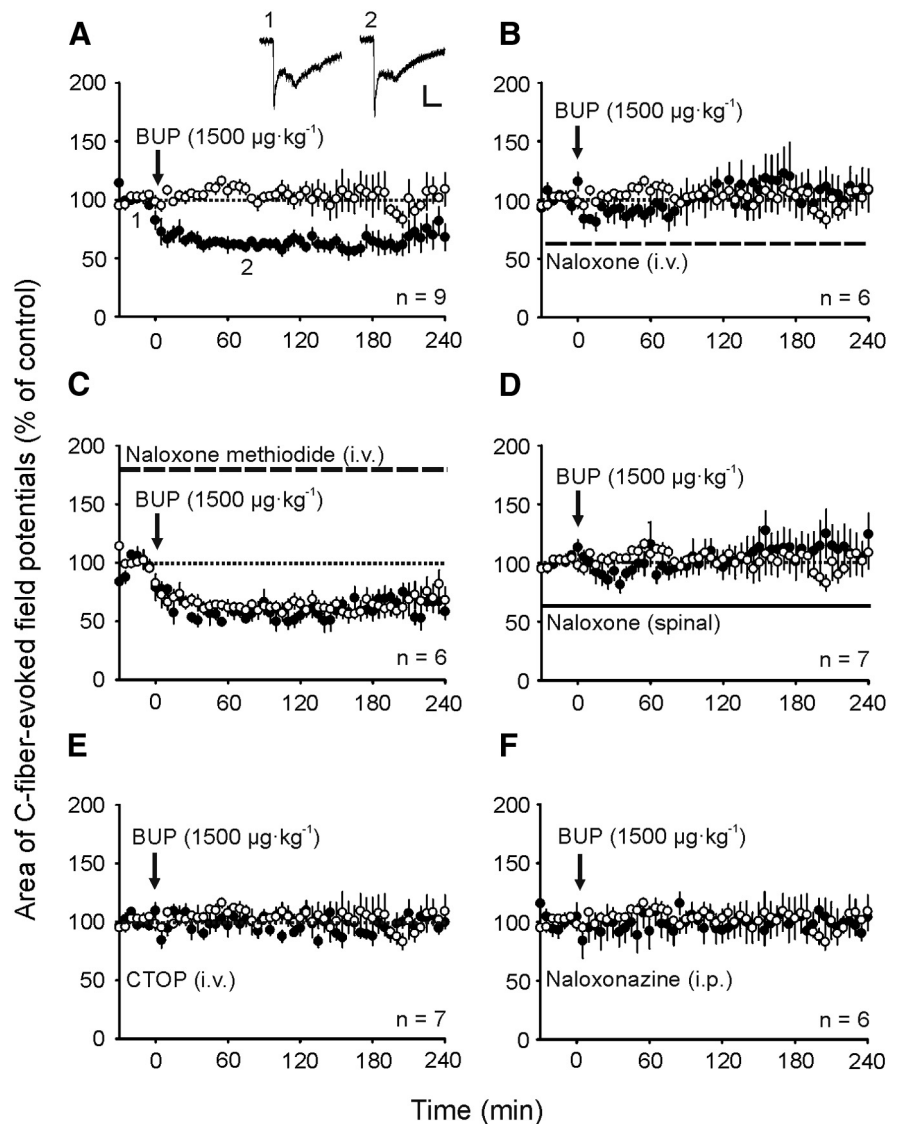


Figure 2. An analgesic dose of buprenorphine depresses strength at C-fiber synapses in the superficial spinal dorsal horn involving the activation of spinal μ_1 -opioid receptors. In all graphs, areas of C-fiber-evoked field potentials were normalized to baseline recording (dotted line) and plotted against time (minutes). **A**, A single intravenous bolus injection of buprenorphine (time point zero, black arrow, $1500 \mu\text{g}\cdot\text{kg}^{-1}$) at an analgesically active dose significantly depressed synaptic strength. Insets show individual traces of field potentials recorded at indicated time points. Scale bars, 100 ms and 0.5 mV. **B**, Continuous intravenous administration of naloxone hydrochloride (dashed black bar, $100 \mu\text{g}\cdot\text{kg}^{-1}\cdot\text{h}^{-1}$) starting 60 min before buprenorphine injection (black arrow, dosing as in **A**) inhibited buprenorphine-induced synaptic depression. **C**, Continuous intravenous infusion of the peripherally restricted naloxone methiodide (dashed black bar, $20 \text{mg}\cdot\text{kg}^{-1}\cdot\text{h}^{-1}$) starting 60 min before buprenorphine injection (black arrow, dosing as in **A**) had no effect on buprenorphine-induced synaptic depression. **D**, Spinal superfusion with naloxone hydrochloride (black bar, $100 \mu\text{M}$) prevented synaptic depression induced by buprenorphine bolus injection (black arrow, dosing as in **A**). **E**, Systemic administration of the selective μ_1 -opioid receptor antagonist CTOP ($1 \text{mg}\cdot\text{kg}^{-1}$) applied 60 min before buprenorphine bolus injection (black arrow, dosing as in **A**) prevented synaptic depression. **F**, Similarly, systemic application of the selective μ_1 -opioid receptor antagonist naloxonazine ($10 \text{mg}\cdot\text{kg}^{-1}$), injected intraperitoneally 24 h before buprenorphine (black arrow, dosing as in **A**), abolished depression of synaptic strength. For **A–F**, time courses of buprenorphine-treated animals are shown in black circles. Data are expressed as mean \pm SEM. Statistics: **A, B, D, E, F**, Two-way ANOVA versus untreated controls (open circles), followed by Bonferroni *post hoc* test; **A**: $F_{(1,17)} = 437.8, p < 0.0001$; **B**: $F_{(1,53)} = 0.232, p = 0.629$; **D**: $F_{(1,607)} = 0.36, p = 0.549$; **E**: $F_{(55,605)} = 0.6858, p = 0.959$; **F**: $F_{(1,55)} = 1.148, p = 0.285$; **C**, two-way ANOVA versus buprenorphine (open circles) followed by Bonferroni *post hoc* test; **C**: $F_{(1,725)} = 9.672, p = 0.0019$.

statistical differences in the ANOVA, there are no significant differences when individual time points are tested with *post hoc* tests.

The sample size of each electrophysiological and immunohistochemical experimental group is given in the Results section and can be found in the respective figures. The sample size of each behavioral experimental group is provided in Table 2 and the respective figure legends.

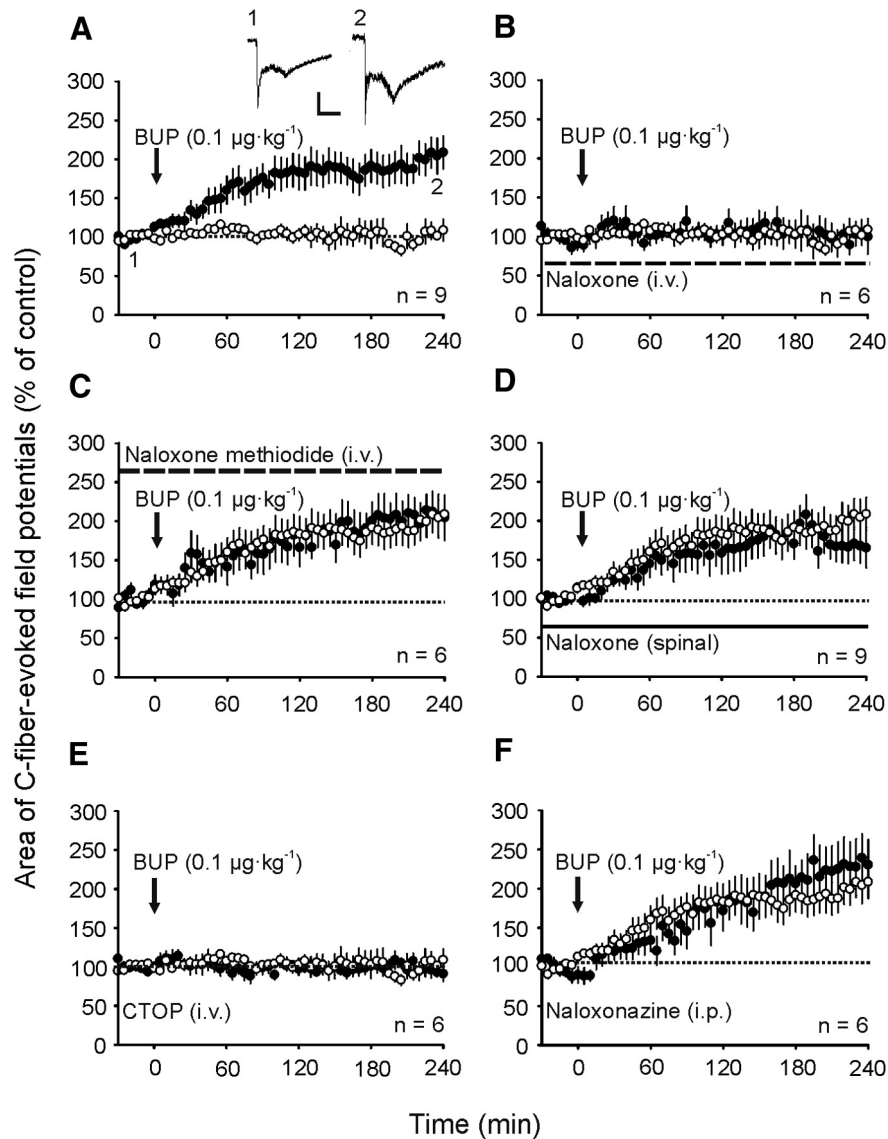


Figure 3. Ultra-low-dose buprenorphine induces facilitation of strength at C-fiber synapses in the superficial spinal dorsal horn via the activation of supraspinal naloxonazine-insensitive μ -opioid receptors. In all graphs, areas of C-fiber-evoked field potentials were normalized to baseline recording (dotted line) and plotted against time (minutes). **A**, Time course of the facilitation of synaptic strength by ultra-low-dose buprenorphine ($0.1 \mu\text{g}\cdot\text{kg}^{-1}$) administered as a single intravenous bolus injection at time point zero (black arrow). Insets show individual traces of field potentials recorded at indicated time points. Scale bars, 100 ms and 0.5 mV. **B**, Intravenous infusion of naloxone hydrochloride (dashed black bar, $100 \mu\text{g}\cdot\text{kg}^{-1}\cdot\text{h}^{-1}$) starting 60 min before buprenorphine injection (black arrow, dosing as in **A**) and lasting throughout the recording period prevented synaptic facilitation by ultra-low-dose buprenorphine. **C**, Continuous intravenous infusion of naloxone methiodide (dashed black bar, $20 \text{mg}\cdot\text{kg}^{-1}\cdot\text{h}^{-1}$) starting 60 min before buprenorphine injection (black arrow, dosing as in **A**) had no effect on ultra-low-dose buprenorphine-induced synaptic facilitation. **D**, Spinal superfusion with naloxone hydrochloride (black bar, $100 \mu\text{M}$) throughout the recording period failed to prevent synaptic facilitation by ultra-low-dose buprenorphine (black arrow, dosing as in **A**). **E**, Systemic administration of CTOP ($1 \text{mg}\cdot\text{kg}^{-1}$) applied 60 min before ultra-low-dose buprenorphine bolus injection (black arrow, dosing as in **A**) prevented synaptic facilitation. **F**, In contrast, naloxonazine (dosing as in **A**) had no effect on the facilitation of synaptic strength by ultra-low-dose buprenorphine (black arrow, dosing as in **A**)-induced facilitation of synaptic strength. For **A–F**, time courses of buprenorphine-treated animals are shown in black circles. Data are expressed as mean \pm SEM. Statistics: **A, B, E**, two-way ANOVA versus untreated controls (open circles) followed by Bonferroni *post hoc* test; **A**: $F_{(1,719)} = 364.3, p < 0.0001$; **B**: $F_{(1,528)} = 0.561, p = 0.454$; **E**: $F_{(1,548)} = 2.451, p = 0.118$; **C, D, F**, two-way ANOVA versus ultra-low-dose buprenorphine (open circles) followed by Bonferroni *post hoc* test; **C**: $F_{(1,719)} = 0.096, p = 0.757$; **D**: $F_{(1,879)} = 12.78, p = 0.0004$; **F**: $F_{(1,728)} = 0.108, p = 0.742$.

Results

Acute bolus application of buprenorphine has analgesic effects but a 15,000-fold lower dose induces mechanical and thermal hyperalgesia

In rodents, buprenorphine at a dose of $1500 \mu\text{g}\cdot\text{kg}^{-1}$, which is close to the median effective dose in rats obtained from tail-flick

experiments (Cowan et al., 1977), typically produces analgesia in behavioral assays (Christoph et al., 2005). In the present study, intraperitoneal injection of buprenorphine ($1500 \mu\text{g}\cdot\text{kg}^{-1}$) increased response latencies to a high-intensity radiant heat stimulus compared with vehicle-treated animals for at least 6 h (Fig. 1A). We next examined the responses to mechanical and thermal stimuli before and after intraperitoneal injection of buprenorphine at a 15,000-fold lower dose ($0.1 \mu\text{g}\cdot\text{kg}^{-1}$). At this ultra-low dose, buprenorphine significantly diminished the response latencies to a low-intensity radiant heat stimulus compared with vehicle-treated animals (Fig. 1B). At 24 h after injection, buprenorphine-induced thermal hyperalgesia had vanished (Fig. 1B). Buprenorphine also decreased the response thresholds to von Frey filaments compared with vehicle control (Fig. 1C). In buprenorphine-treated animals, mechanical hyperalgesia was dissolved 24 h after the injection (Fig. 1C). Response values and statistics are shown in Table 2. Together, these experiments demonstrate that buprenorphine induces qualitatively different effects on nociception over a dose range spanning four orders of magnitude.

At an analgesic dose systemic buprenorphine depresses strength at spinal C-fiber synapses via activation of spinal naloxonazine-sensitive μ_1 -opioid receptors

We next investigated whether analgesia by buprenorphine at $1500 \mu\text{g}\cdot\text{kg}^{-1}$ intravenous is associated with an effect on synaptic transmission in the spinal cord dorsal horn. At this dose, buprenorphine significantly depressed the area of C-fiber-evoked field potentials (to $68 \pm 11\%$ of baseline at 240 min, $p = 0.03$ vs untreated controls, $n = 9$; Fig. 2A) after a single bolus injection. Continuous intravenous infusion of the broad-spectrum opioid receptor antagonist naloxone hydrochloride ($100 \mu\text{g}\cdot\text{kg}^{-1}\cdot\text{h}^{-1}$) starting 60 min before buprenorphine injection and lasting throughout the recording period fully prevented synaptic depression ($108 \pm 18\%$ of baseline at 240 min, $p = 1$ vs untreated controls, $n = 6$; Fig. 2B) until the end of the recording period. In contrast, intravenous infusion of naloxone methiodide ($20 \text{mg}\cdot\text{kg}^{-1}\cdot\text{h}^{-1}$), which does not cross the blood–CNS barrier, did not prevent buprenorphine-induced inhibition of synaptic strength ($58 \pm 7\%$ of baseline at 240 min, $p = 1$ vs buprenorphine alone, $n = 6$; Fig. 2C). Spinal application of naloxone methiodide (1 mM), however, fully blocked buprenorphine-induced synaptic depres-

sion in all 7 animals tested (data not shown). Likewise, when we applied naloxone hydrochloride ($100 \mu\text{M}$) 60 min before buprenorphine injection directly onto the spinal cord at the recording site, systemic buprenorphine no longer depressed synaptic strength ($124 \pm 18\%$ of baseline at 240 min, $p = 1$ vs untreated controls, $n = 7$; Fig. 2D). Naloxone has been shown to also have antagonistic effects on TLR4s (Hutchinson et al., 2008). The contribution of these receptors to buprenorphine-induced effects on synaptic strength can thus not be excluded at this point. We next used CTOP to selectively block μ -opioid receptors. Intravenous bolus injection of CTOP ($1 \text{ mg}\cdot\text{kg}^{-1}$) 60 min before buprenorphine fully prevented buprenorphine-induced inhibition of synaptic strength ($100 \pm 5\%$ of baseline at 240 min, $p = 1$ vs untreated controls, $n = 7$; Fig. 2E). Our data indicate that, despite a reported low blood–CNS barrier permeability (Van Dorpe et al., 2010), CTOP reached a sufficiently high concentration in the CNS to block central μ -opioid receptors under our experimental conditions. We next used naloxonazine to selectively block μ_1 -opioid receptors. It has been reported that, initially, naloxonazine might bind reversibly to other opioid receptor subtypes. Therefore, it is commonly applied 24 h before treatment to secure μ_1 specificity (Hahn and Pasternak, 1982; Ling et al., 1986; Pasternak and Pan, 2013). A single intraperitoneal bolus injection of naloxonazine ($10 \text{ mg}\cdot\text{kg}^{-1}$) 24 h before buprenorphine administration fully prevented buprenorphine-induced depression of synaptic strength ($104 \pm 16\%$ of baseline at 240 min, $p = 1$ vs untreated controls, $n = 6$; Fig. 2F). Intravenous injection of naloxonazine 60 min before buprenorphine administration revealed the same results in all six animals tested (data not shown). Collectively, these data suggest that buprenorphine-induced inhibition of synaptic strength is mediated by spinal opioid receptors of the μ_1 subtype.

Facilitation of synaptic strength by ultra-low-dose buprenorphine depends on supraspinal CTOP-sensitive but naloxonazine-insensitive μ -opioid receptors

We next studied the pronociceptive mechanisms of ultra-low-dose buprenorphine. A single intravenous bolus injection of buprenorphine at a dose of $0.1 \mu\text{g}\cdot\text{kg}^{-1}$ immediately elicited a slowly rising and long-lasting synaptic facilitation in the spinal cord dorsal horn (to $209 \pm 21\%$ of baseline at 240 min, $p = 0.001$ vs untreated controls, $n = 9$; Fig. 3A). Continuous intravenous naloxone hydrochloride administration ($100 \mu\text{g}\cdot\text{kg}^{-1}\cdot\text{h}^{-1}$) starting 60 min before buprenorphine injection and lasting throughout the recording period abolished ultra-low-dose buprenorphine-induced facilitation of synaptic strength ($100 \pm 22\%$ of baseline at 240 min, $p = 1$ vs untreated controls, $n = 6$; Fig. 3B). In contrast, continuous intravenous infusion of naloxone methiodide ($20 \text{ mg}\cdot\text{kg}^{-1}\cdot\text{h}^{-1}$) did not affect ultra-low-dose buprenorphine-induced synaptic facilitation ($204 \pm 29\%$ of baseline at 240 min, $p = 1$ vs ultra-low-dose buprenorphine, $n = 6$; Fig. 3C). Likewise, topical administration of naloxone hydrochloride ($100 \mu\text{M}$) onto the spinal cord 60 min before buprenorphine injection failed to prevent synaptic facilitation by ultra-low-dose buprenorphine ($165 \pm 26\%$ of baseline at 240 min, $p = 1$ vs ultra-low-dose buprenorphine, $n = 9$; Fig. 3D). Together, our data indicate that ultra-low-dose buprenorphine-induced facilitation is independent of peripheral and spinal naloxone-sensitive receptors. Blockade of μ -opioid receptors with CTOP ($1 \text{ mg}\cdot\text{kg}^{-1}$) injected intravenously 60 min before ultra-low-dose buprenorphine, however, abolished facilitation of synaptic strength ($91 \pm$

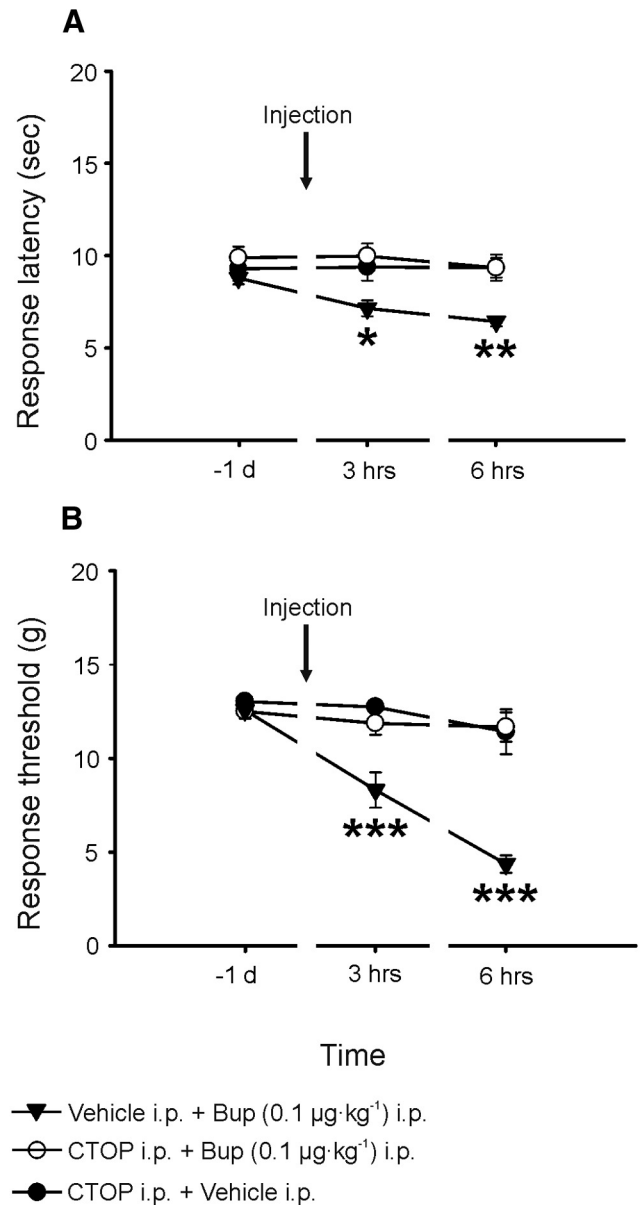


Figure 4. Mechanical and thermal hyperalgesia induced by ultra-low-dose buprenorphine require activation of μ -opioid receptors. Animals received an intraperitoneal injection of CTOP or 0.9% sterile saline 60 min before intraperitoneal bolus injection of buprenorphine (black arrow) under short isoflurane anesthesia. Control animals received CTOP intraperitoneally followed by an intraperitoneal vehicle injection (black circles). **A**, Mean response thresholds to radiant heat stimulation are plotted at different time points. Animals pretreated with systemic CTOP ($1 \text{ mg}\cdot\text{kg}^{-1}$) failed to develop thermal hyperalgesia upon ultra-low-dose buprenorphine administration ($0.1 \mu\text{g}\cdot\text{kg}^{-1}$, open circles, $n = 9$). Buprenorphine ($0.1 \mu\text{g}\cdot\text{kg}^{-1}$, black triangle, $n = 7$) reduced mean response latencies to heat stimulation of the hindpaw compared with vehicle control animals (black circles, $n = 8$). Response latencies in the vehicle control group (black circles) remained stable. **B**, The mean response thresholds to probing with von Frey filaments are plotted at different time points. Systemic injection of CTOP (dosing as in **A**, open circles, $n = 9$) fully prevented development of ultra-low-dose buprenorphine-induced mechanical hyperalgesia. Ultra-low-dose buprenorphine (dosing as in **A**, black triangle, $n = 7$) reduced mean von Frey thresholds compared with vehicle control (black circles, $n = 8$). In the control group, response thresholds remained stable (black circles). Statistics: **A**, **B**, two-way ANOVA vs control group (black circles) followed by Bonferroni *post hoc* test; p - and F -values are listed in Table 1. * $p < 0.05$, ** $p < 0.01$, *** $p < 0.001$.

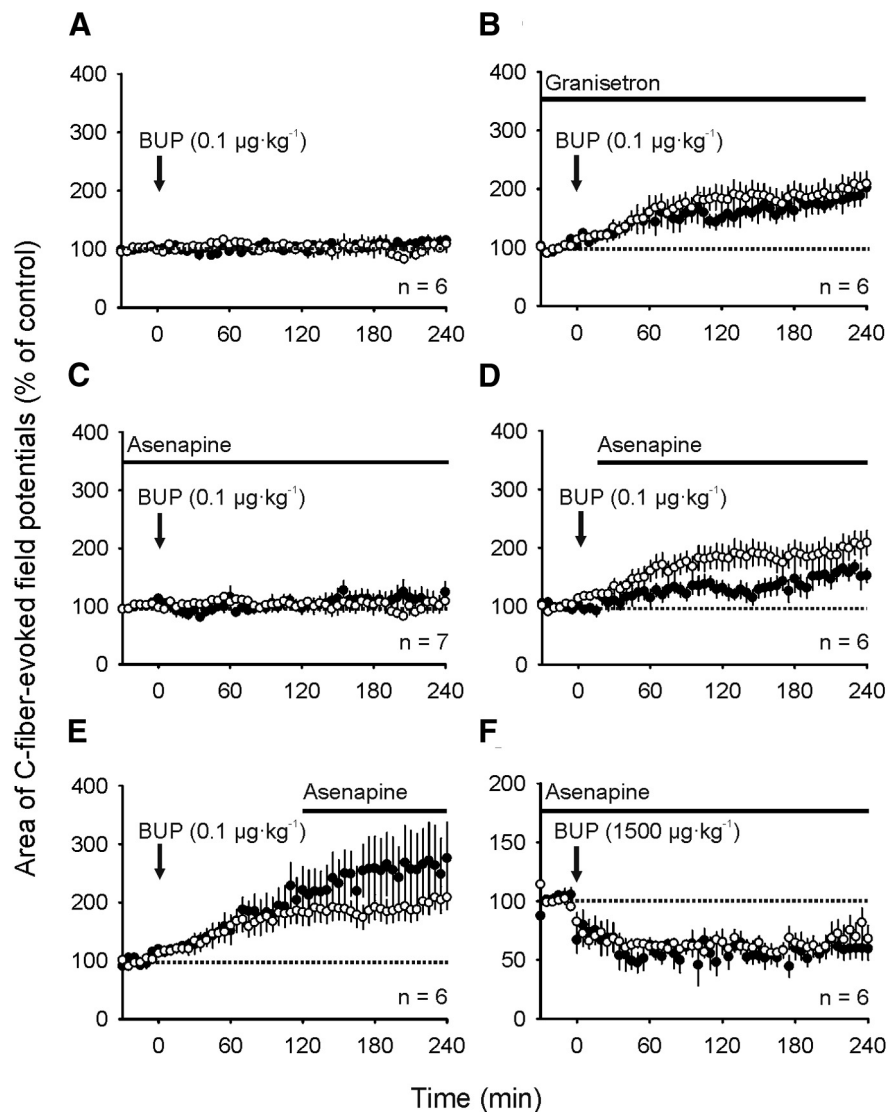


Figure 5. Facilitation of synaptic strength induced by ultra-low-dose buprenorphine involves activation of descending, monoaminergic pathways. In all graphs, areas of C-fiber-evoked field potentials were normalized to baseline recording (dotted line) and plotted against time (minutes). **A**, Surgical disruption of descending pathways by spinalization at the cervical level 3 h before buprenorphine injection (black arrow, $0.1 \mu\text{g}\cdot\text{kg}^{-1}$) prevented development of synaptic facilitation. **B**, Continuous superfusion of the 5-HT₃R antagonist granisetron (black bar, 1 mM) starting 60 min before buprenorphine injection (black arrow, dosing as in **A**) failed to prevent ultra-low-dose buprenorphine-induced synaptic facilitation. **C**, Continuous spinal superfusion with the antipsychotic drug asenapine maleate (black bar, 5 μM) throughout the recording time inhibited synaptic facilitation induced by intravenous ultra-low-dose buprenorphine (black arrow, dosing as in **A**). **D, E**, Ultra-low-dose buprenorphine-induced facilitation of synaptic strength was significantly reduced when asenapine (black bar, dosing as in **A**) was applied to the spinal cord 15 min (**D**) but not 2 h after buprenorphine injection (**E**; black arrow, dosing as in **A**). **F**, Asenapine (black bar) had no effect on buprenorphine (black arrow, $1500 \mu\text{g}\cdot\text{kg}^{-1}$)-induced depression of synaptic strength. For **A–D**, Time courses of buprenorphine-treated animals are shown in black circles. Data are expressed as mean \pm SEM. Statistics: **A, C**, two-way ANOVA versus untreated controls (open circles) followed by Bonferroni *post hoc* test; **A**: $F_{(1,551)} = 0.034, p = 0.854$; **C**: $F_{(1,601)} = 0.521, p = 0.47$; **B, D, E**, two-way ANOVA vs ultra-low-dose buprenorphine (open circles) followed by Bonferroni *post hoc* test; **B**: $F_{(1,728)} = 14.84, p < 0.0001$; **D**: $F_{(1,722)} = 119.5, p < 0.0001$; **E**: $F_{(1,727)} = 34.49, p < 0.0001$; **F**: two-way ANOVA vs analgesic-dose buprenorphine (open circles) followed by Bonferroni *post hoc* test, $F_{(1,723)} = 14.01, p = 0.0002$.

10% of baseline at 240 min, $p = 1$ vs untreated controls, $n = 6$; Fig. 3E). Synaptic facilitation was also prevented by an intravenous bolus injection of the μ -opioid receptor antagonist CTAP ($1 \text{ mg}\cdot\text{kg}^{-1}$) 60 min before ultra-low-dose buprenorphine administration in all three animals tested (data not shown). In contrast, selective blockade of μ_1 -opioid receptors with naloxonazine ($10 \text{ mg}\cdot\text{kg}^{-1}$) 24 h before buprenorphine administration failed to impede ultra-low-dose buprenorphine-induced synaptic facilitation ($230 \pm 24\%$ of base-

line at 240 min, $p = 1$ vs ultra-low-dose buprenorphine, $n = 6$; Fig. 3F). Intravenous injection of naloxonazine 60 min before buprenorphine administration revealed the same results in all six animals tested (data not shown). Collectively, these data indicate that ultra-low-dose buprenorphine induces synaptic facilitation via activation of supraspinal CTOP-sensitive but naloxonazine-insensitive μ -opioid receptors.

Systemically applied CTOP abolishes ultra-low-dose buprenorphine-induced mechanical and thermal hyperalgesia

Because CTOP fully prevented ultra-low-dose buprenorphine-induced synaptic facilitation, we next investigated whether systemic blockade of μ -opioid receptors also affects mechanical and thermal hyperalgesia induced by ultra-low-dose buprenorphine. Indeed, the increase in withdrawal latency upon noxious heat stimulation after ultra-low-dose buprenorphine ($0.1 \mu\text{g}\cdot\text{kg}^{-1}$) administration was fully prevented by systemic pretreatment with CTOP ($1 \text{ mg}\cdot\text{kg}^{-1}$; Fig. 4A). Similarly, the same pretreatment with CTOP completely inhibited ultra-low-dose buprenorphine-induced reduction in paw withdrawal thresholds to stimulation with von Frey filaments (Fig. 4B). Response values and statistics are shown in Table 2. These data suggest that ultra-low-dose buprenorphine-induced mechanical and thermal hyperalgesia involve the activation of CTOP-sensitive μ -opioid receptors.

Ultra-low-dose buprenorphine activates descending monoaminergic pathways

We next investigated whether descending pathways arising from supraspinal areas mediate the facilitating effects in the spinal cord of systemically applied ultra-low-dose buprenorphine. We surgically disrupted descending pathways at the C6–C7 level by thermal cautery 3 h before injecting buprenorphine. Spinalization fully prevented synaptic facilitation by ultra-low-dose buprenorphine ($0.1 \mu\text{g}\cdot\text{kg}^{-1}$; $115 \pm 7\%$ of baseline at 240 min, $p = 1$ vs untreated controls, $n = 6$; Fig. 5A). We have shown previously that descending facilitation induced by fentanyl or morphine is mediated by spinal 5-HT₃Rs (Heinl et al., 2011). To determine whether similar mechanisms account for ultra-low-dose buprenorphine-induced facilitation of synaptic strength, we blocked spinal 5-HT₃Rs by topical application of granisetron (1 mM), a selective 5-HT₃R antagonist. However, this treatment failed to affect synaptic facilitation by ultra-low-dose buprenorphine ($202 \pm 17\%$ of baseline at 240 min, $p = 1$ vs ultra-low-dose buprenorphine, $n = 6$; Fig. 5B). To determine

whether ultra-low-dose buprenorphine elicits the activation of other monoamine receptors, we applied the broad-spectrum serotonin, noradrenaline, dopamine, and histamine receptor antagonist asenapine ($5 \mu\text{M}$), which has no effect on ionotropic $5\text{-HT}_3\text{Rs}$, directly onto the spinal cord dorsum. In the presence of asenapine, ultra-low-dose buprenorphine failed to facilitate synaptic strength, which remained stable over the whole recording period of 4 h ($105 \pm 9\%$ of baseline 240 min, $p = 1$ vs untreated controls, $n = 6$; Fig. 5C). When asenapine was applied at the spinal recording site 15 min after ultra-low-dose buprenorphine bolus injection, synaptic facilitation was significantly reduced (two-way ANOVA vs ultra-low-dose buprenorphine-treated animals, $p < 0.001$) but not fully prevented, although this did not reach statistical significance at 240 min (two-way ANOVA vs untreated controls, $p < 0.001$; $152 \pm 12\%$ of baseline at 240 min, $p = 0.7038$, $n = 6$; Fig. 5D). In contrast, when applied 2 h after ultra-low-dose buprenorphine injection, asenapine no longer had any effect on the development of synaptic facilitation (to $276 \pm 62\%$ of baseline at 240 min, $p = 1$ vs ultra-low-dose buprenorphine, $n = 6$; Fig. 5E). This finding suggests that, shortly after ultra-low-dose buprenorphine injection, monoamines are released from descending neurons, leading to synaptic facilitation in the spinal dorsal horn. If the analgesic dose of buprenorphine likewise activated descending, monoaminergic, facilitating pathways, then one would expect that blocking descending facilitation unmasks the full efficacy of inhibition. However, asenapine had no detectable effect on buprenorphine-induced depression of synaptic transmission ($60 \pm 9\%$ of baseline at 240 min, $p = 1$ compared with the analgesic dose of buprenorphine without asenapine, $n = 6$; Fig. 5F). This suggests that the ultra-low dose but not the analgesic dose of buprenorphine activates descending monoaminergic pathways.

Ultra-low-dose buprenorphine-induced enhancement of synaptic transmission is mediated by coactivation of spinal $5\text{-HT}_{2\text{A}}\text{Rs}$, $5\text{-HT}_{2\text{B}}\text{Rs}$, and $5\text{-HT}_{2\text{C}}\text{Rs}$

One of the $5\text{-HT}_2\text{R}$ subtypes inhibited by asenapine is the $5\text{-HT}_2\text{R}$ (Shahid et al., 2009), which is subclassified into $5\text{-HT}_{2\text{A}}\text{Rs}$, $5\text{-HT}_{2\text{B}}\text{Rs}$, and $5\text{-HT}_{2\text{C}}\text{Rs}$ (Hoyer et al., 1994). To evaluate the contribution of these receptors to ultra-low-dose buprenorphine-induced facilitation of synaptic strength we applied the selective $5\text{-HT}_{2\text{A}}\text{R}$, $5\text{-HT}_{2\text{B}}\text{R}$, and $5\text{-HT}_{2\text{C}}\text{R}$ antagonists 4F 4PP ($200 \mu\text{M}$), SB 204741 ($100 \mu\text{M}$), and RS 102221 (100 nM) onto the spinal cord at the recording site either separately or combined. None of the three drugs alone abolished ultra-low-dose buprenorphine-induced synaptic facilitation (4F 4PP: $152 \pm 18\%$ of baseline 240 min, $p = 1$, $n = 6$, Fig. 6A; SB 204741: $172 \pm 39\%$ of baseline at 240 min, $p = 1$, $n = 6$, Fig. 6B; RS 102221: $146 \pm 23\%$ of baseline at 240

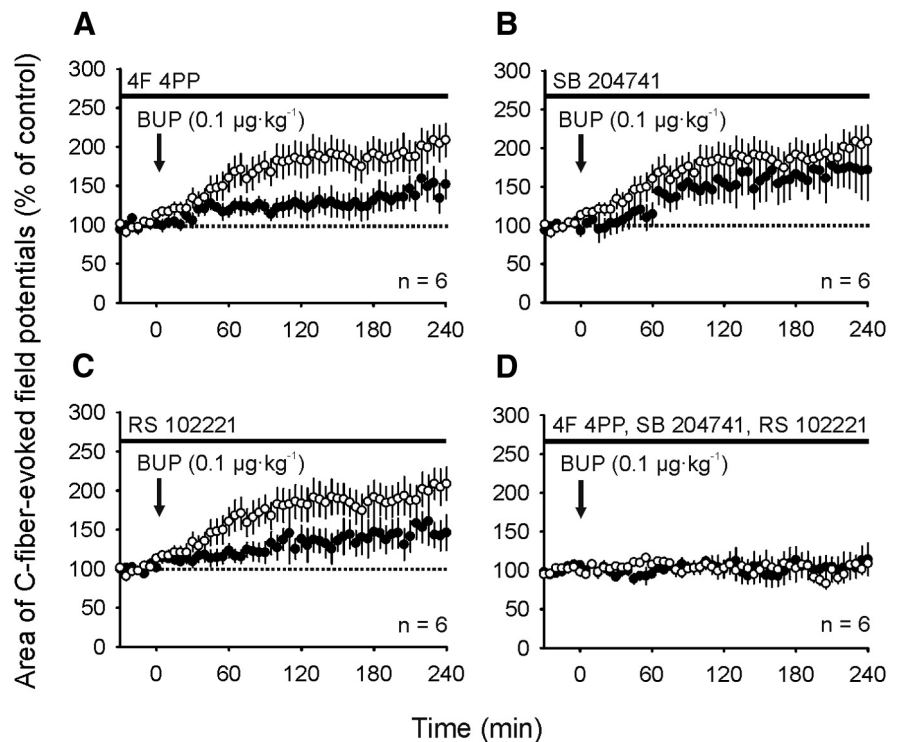


Figure 6. Ultra-low-dose buprenorphine facilitates strength at spinal C-fiber synapses via activation of descending serotonergic pathways. In all graphs, areas of C-fiber-evoked field potentials were normalized to baseline recording (dotted line) and plotted against time (minutes). **A**, Spinal application of the selective $5\text{-HT}_{2\text{A}}\text{R}$ antagonist 4F 4PP (black bar, $200 \mu\text{M}$) significantly reduced facilitation of synaptic strength induced by ultra-low-dose buprenorphine (black arrow, $0.1 \mu\text{g}\cdot\text{kg}^{-1}$). **B**, The selective $5\text{-HT}_{2\text{B}}\text{R}$ antagonist SB 204741 (black bar, $100 \mu\text{M}$) significantly decreased ultra-low-dose buprenorphine-induced synaptic facilitation. **C**, The selective $5\text{-HT}_{2\text{C}}\text{R}$ antagonist RS 102221 (black bar, 100 nM) significantly reduced synaptic facilitation by ultra-low-dose buprenorphine (black arrow, dosing as in **A**). **D**, Combined spinal application of 4F 4PP, SB 204741 and RS 102221 (black bar, dosing as in **A–C**, respectively) completely prevented ultra-low-dose buprenorphine-induced facilitation of synaptic strength. For **A–C**, time courses of buprenorphine-treated animals are shown in black circles. Data are expressed as mean \pm SEM. Statistics: **A–C**, two-way ANOVA versus ultra-low-dose buprenorphine (open circles) followed by Bonferroni *post hoc* test; **A**: $F_{(1,727)} = 151$, $p < 0.0001$; **B**: $F_{(1,726)} = 38.62$, $p < 0.0001$; **C**: $F_{(1,728)} = 110.2$, $p < 0.0001$; **D**: two-way ANOVA vs untreated controls (open circles) followed by Bonferroni *post hoc* test, $F_{(1,718)} = 0.038$, $p = 0.846$.

min, $p = 0.7544$, $n = 6$, Fig. 6C, all compared with ultra-low-dose buprenorphine). Only the combined application of 4F 4PP, SB 204741, and RS 102221 completely inhibited facilitation of synaptic strength by ultra-low-dose buprenorphine ($114 \pm 21\%$ of baseline at 240 min, $p = 1$ vs untreated controls, $n = 9$; Fig. 6D).

Ultra-low-dose buprenorphine-induced hyperalgesia is dependent on activation of spinal $5\text{-HT}_2\text{Rs}$

We next investigated whether $5\text{-HT}_2\text{R}$ blockade also prevents ultra-low-dose buprenorphine-induced thermal and mechanical hyperalgesia. Intrathecal injection of the $5\text{-HT}_{2\text{A}}\text{R}$, $5\text{-HT}_{2\text{B}}\text{R}$, and $5\text{-HT}_{2\text{C}}\text{R}$ antagonists 4F 4PP (2 mM), SB 204741 (1 mM), and RS 102221 ($1 \mu\text{M}$) 15 min before intraperitoneal injection of buprenorphine at $0.1 \mu\text{g}\cdot\text{kg}^{-1}$ fully prevented the increase in withdrawal latency upon noxious heat stimulation induced by ultra-low-dose buprenorphine injection (Fig. 7A). Similarly, intrathecal treatment with $5\text{-HT}_2\text{R}$ antagonists completely inhibited ultra-low-dose buprenorphine-induced reduction in paw withdrawal thresholds to stimulation with von Frey filaments (Fig. 7B). Response values and statistics are shown in Table 2.

$5\text{-HT}_2\text{R}$ activation induces calcium increase in dorsal horn astrocytes

Because $5\text{-HT}_2\text{Rs}$ are expressed on astrocytes in the spinal cord (Maxishima et al., 2001), we next investigated whether activation

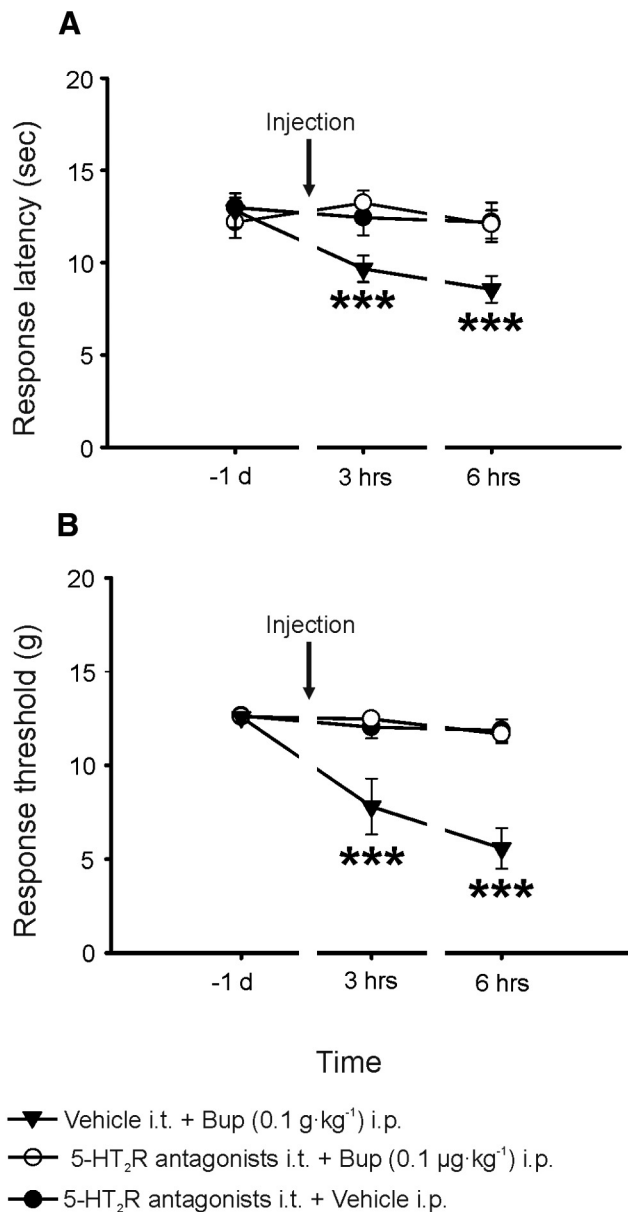


Figure 7. Spinal 5-HT₂R blockade fully prevents ultra-low-dose buprenorphine-induced hyperalgesia. Animals received an intrathecal injection of the 5-HT_{2A}R, 5-HT_{2B}R, and 5-HT_{2C}R antagonists 4F 4PP, SB 204741, and RS 102 221 or 25% DMSO/NaCl vehicle 15 min before intraperitoneal bolus injection of buprenorphine or saline (black arrow) under isoflurane anesthesia. Control animals received antagonists intrathecally followed by an intraperitoneal vehicle injection (black circle). **A**, The mean response thresholds to radiant heat stimulation are plotted at different time points. Ultra-low-dose buprenorphine (0.1 μg·kg⁻¹, black triangle, $n = 9$) reduced mean response latencies to heat stimulation of the hindpaw compared with control (black circles, $n = 8$). Animals treated with intrathecally injected 5-HT₂R antagonists 4F 4PP (2 mM), SB 204741 (1 mM), and RS 102221 (1 μM, open circles, $n = 9$) failed to develop hyperalgesia after ultra-low-dose buprenorphine injection. Response latencies in the control group (black circles) remained stable. **B**, Mean response thresholds to probing with von Frey filaments are plotted at different time points. Ultra-low-dose buprenorphine (dosing as in **A**, black triangle, $n = 9$) reduced mean von Frey thresholds compared with vehicle control (black circles, $n = 8$). Intrathecal injection of 5-HT₂R antagonists (dosing as in **A**, open circles, $n = 9$) fully prevented development of ultra-low-dose buprenorphine-induced hyperalgesia. In the control group, response thresholds remained stable (black circles). Statistics: **A**, **B**, two-way ANOVA versus control group (black circles) followed by Bonferroni *post hoc* test; p - and F -values are listed in Table 1. *** $p < 0.001$.

of 5-HT_{2A}Rs, 5-HT_{2B}Rs, and 5-HT_{2C}Rs has an effect on calcium signaling in spinal astrocytes.

In a slice preparation of the rat lumbar spinal cord puff application of the selective 5-HT_{2A}Rs, 5-HT_{2B}Rs, and 5-HT_{2C}R agonists TCB-2, BW 723C86, and CP 809101 (all 5 mM) in the presence of tetrodotoxin to inhibit neuronal action potential firing, 11/16 astrocytes ($n = 16$ cells in 9 experiments) exhibited clear increases in Fluo-5F fluorescence intensity (range in amplitude 20–256% of baseline fluorescence). The mean increase in all 16 recorded astrocytes was $70 \pm 21\%$ (Fig. 8B). In the presence of the specific 5-HT_{2A}R, 5-HT_{2B}R, and 5-HT_{2C}R antagonists 4F 4PP (200 μM), SB 204741 (100 μM), and RS 102221 (100 nM), a clear fluorescence increase was observed in only 3/17 astrocytes ($n = 17$ cells in 8 experiments, range 23–80% of baseline fluorescence intensity). The mean fluorescence increase during inhibition of 5-HT_{2A}Rs, 5-HT_{2B}Rs, and 5-HT_{2C}Rs was $11 \pm 6\%$ (Fig. 8B). Both the number of responding cells ($p = 0.009$) and the amplitude of responses ($p = 0.003$) were significantly reduced by the specific 5-HT_{2A}R, 5-HT_{2B}R, and 5-HT_{2C}R antagonists. These results demonstrate that astrocytes in the spinal dorsal horn respond to 5-HT₂R activation with a transient increase in the intracellular concentration of free calcium.

Ultra-low-dose buprenorphine leads to an upregulation of the astrocytic marker GFAP

The upregulation of the astrocytic marker GFAP and the microglial marker Iba1 are frequently used to visualize activation of these cells. Immunohistochemical staining revealed a significant increase in normalized GFAP immunoreactivity in ultra-low-dose buprenorphine- (0.1 μg·kg⁻¹) compared with vehicle-treated animals at 6 h after intraperitoneal bolus injection ($315 \pm 25\%$ vs $235 \pm 23\%$, $p = 0.03$, $n = 9$ animals, 12 slices/animal; Fig. 8D). The effect vanished 24 h after buprenorphine injection ($166 \pm 35\%$ vs $185 \pm 38\%$, $p = 0.72$, $n = 6$; Fig. 8D). In contrast, buprenorphine failed to affect normalized Iba1 immunoreactivity (data not shown).

Ultra-low-dose buprenorphine-induced enhancement of synaptic transmission depends on spinal NMDARs and glial cells

We next investigated whether metabolic blockade of spinal glial cells affects ultra-low-dose buprenorphine-induced synaptic facilitation. Indeed, the application of the glial cell toxin fluorocitrate (10 μM) directly on the spinal dorsum entirely averted synaptic facilitation after ultra-low-dose buprenorphine injection (0.1 μg·kg⁻¹; $91 \pm 10\%$ of baseline at 240 min, $p = 1$ vs untreated controls, $n = 6$; Fig. 9A). In addition, when fluorocitrate was applied 2 h after ultra-low-dose buprenorphine injection, synaptic facilitation was fully reversed ($98 \pm 5\%$ at 240 min $p = 1$ vs untreated controls, $n = 6$; Fig. 9B). D-serine is a gliotransmitter and coagonist at NMDARs and may thereby influence synaptic transmission. After topical administration of DAO (1 U/mL), which oxidizes and inactivates D-serine, an overall significant reduction of the curve was observed (two-way ANOVA vs ultra-low-dose buprenorphine treated animals: $p < 0.0001$), although this did not reach statistical significance at the 240 min time point ($150 \pm 17\%$ of baseline at 240 min, Bonferroni *post hoc* comparison: $p = 1$ vs ultra-low-dose buprenorphine, $n = 6$; Fig. 9C).

An increased D-serine release, for example, from spinal astrocytes induced by ultra-low-dose buprenorphine, could lead to enhanced NMDAR activation and thereby to facilitation of synaptic strength. Indeed, topical administration of the com-

petitive NMDAR antagonist D-AP5 (100 μM) abolished synaptic facilitation induced by ultra-low-dose buprenorphine ($118 \pm 5\%$ of baseline 240 min, $p = 1$, compared with untreated controls, $n = 6$; Fig. 9D).

Discussion

The present study demonstrates that, at an analgesic dose, buprenorphine elicited depression of synaptic strength at spinal C-fibers, which involved the activation of spinal, naloxonazine-sensitive μ_1 -opioid receptors. In contrast, at an ultra-low dose, buprenorphine induced facilitation of synaptic strength at C-fibers in the dorsal horn. This required activation of supraspinal, naloxonazine-insensitive μ -opioid receptors, descending serotonergic pathways, and spinal glial cells.

Buprenorphine depresses strength at spinal C-fiber synapses

Buprenorphine is a mixed opioid receptor agonist/antagonist interacting with different opioid receptor subtypes (Lutfy and Cowan, 2004). Its analgesic action has been associated with μ -opioid receptor activation because buprenorphine fails to elicit analgesia in μ -opioid receptor knock-out mice (Lutfy et al., 2003; Ide et al., 2004). It has, however, been controversial whether buprenorphine exerts its antinociceptive effects predominantly by acting on spinal or supraspinal sites (Bryant et al., 1983; Yamamoto et al., 2006). In the present study, a single bolus injection of a high dose of buprenorphine, which induced robust analgesia in behaving animals (Christoph et al., 2005; present study), strongly and persistently depressed C-fiber-evoked field potentials in the dorsal horn. This depression was abolished by pretreatment with either systemically or spinally applied naloxone hydrochloride, by systemically applied CTOP, or by systemically applied naloxonazine, a μ_1 -opioid receptor antagonist (Hahn and Pasternak, 1982; Hahn et al., 1982; Ling et al., 1986). Without excluding any additional supraspinal components, our results clearly suggest that buprenorphine produces analgesia by activating spinal μ_1 -opioid receptors and thereby depressing synaptic strength at C-fibers.

Pronociceptive effects of ultra-low-dose buprenorphine involve supraspinal μ -opioid receptors

The clinical use of opioids might be limited by the development of OIH. It has been thought that buprenorphine would

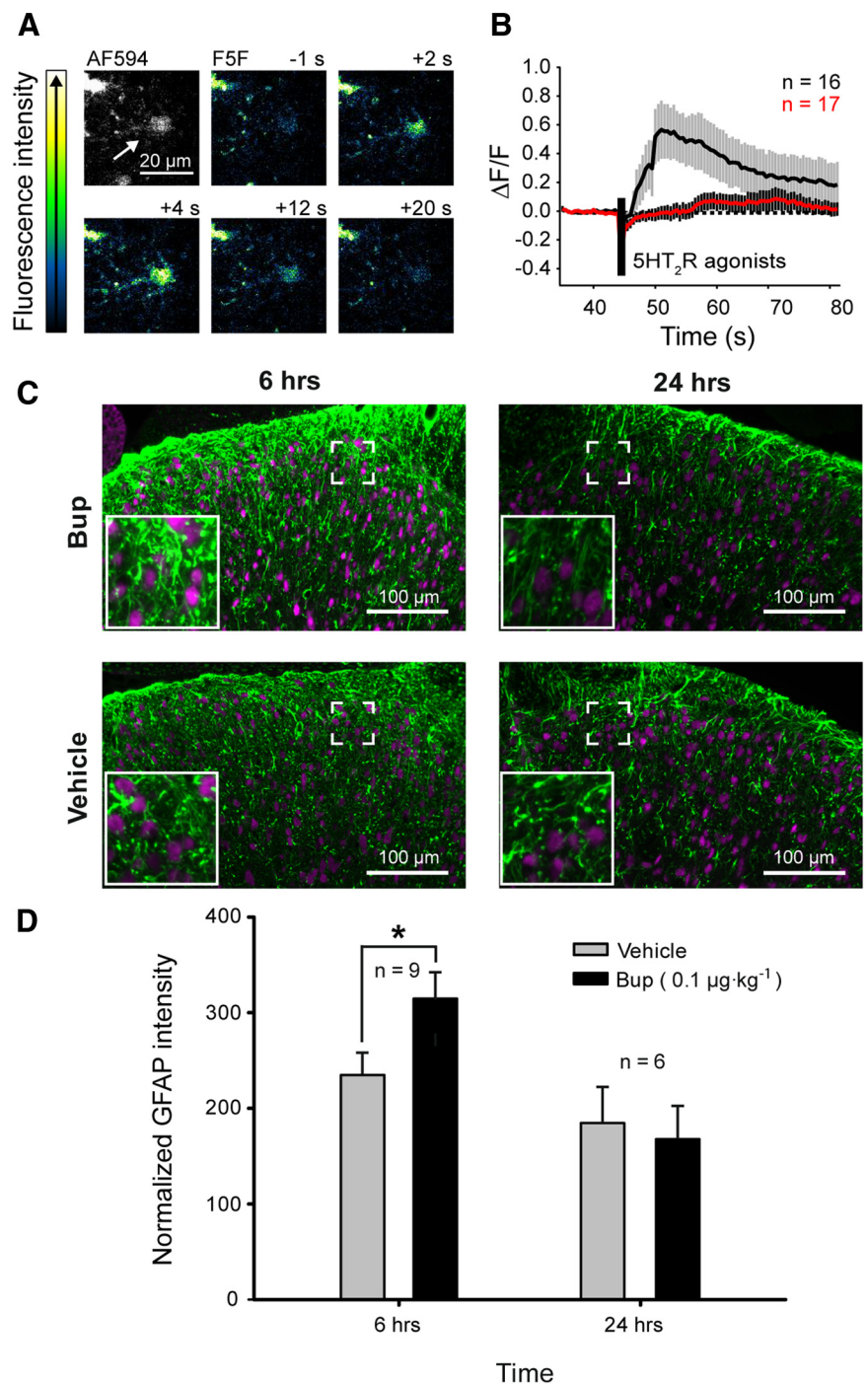


Figure 8. Astrocyte signaling and increased activation state accompany ultra-low-dose buprenorphine effects. **A**, Images of a sample experiment illustrating calcium signaling in spinal dorsal horn astrocytes. Arrow in Alexa Fluor 594 (AF594) image illustrates one of the measured astrocytes. All other images are pseudocolored (see color scale bar on left) indicating changes in F5F fluorescence intensity upon puff application of the 5-HT_{2A}R, 5-HT_{2B}R, and 5-HT_{2C}R agonists (200 ms) 5 mM TCB-2, BW 723C86 and CP 809101). **B**, Average increase in F5F fluorescence intensity of all measured astrocytes normalized to the baseline value ($\Delta F/F$). Application of 5-HT₂R agonists under control conditions is shown in black and application of agonists in the presence of receptor antagonists (200 μM 4F 4PP, 100 μM SB 204741, 100 nM RS 102221) is shown in red. **C, D**, Animals were injected with a single intraperitoneal bolus of buprenorphine (0.1 $\mu\text{g}\cdot\text{kg}^{-1}$) or saline and perfused at 6 or 24 h after treatment. **C**, Immunoreactivity for the astrocyte-specific marker GFAP (green) and the neuronal marker NeuN (magenta). **D**, Mean of GFAP intensity normalized to NeuN intensity in buprenorphine- and vehicle-treated animals. Six hours after buprenorphine injection, GFAP immunofluorescence is increased compared with control animals; 24 h after buprenorphine treatment, GFAP immunoreactivity levels are back to control again.

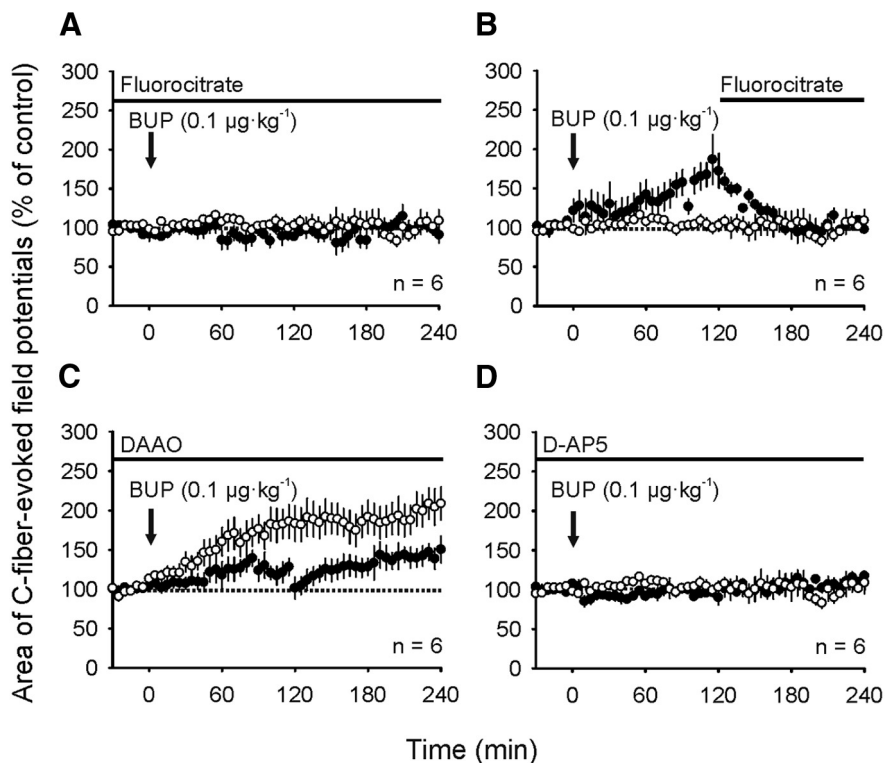


Figure 9. Facilitation of strength at C-fiber synapses by ultra-low-dose buprenorphine depends on spinal glial cells, D-serine, and the activation of spinal NMDARs. Areas of C-fiber-evoked field potentials were normalized to baseline recording (dotted line) and plotted against time (minutes). **A**, The glial toxin fluorocitrate was applied topically to the spinal cord dorsum (black bar, 10 μM), which prevented facilitation of synaptic strength after bolus injection of ultra-low-dose buprenorphine (black arrow, 0.1 $\mu\text{g}\cdot\text{kg}^{-1}$). **B**, When fluorocitrate (black bar, dosing as in **A**) was applied to the spinal cord 2 h after ultra-low-dose buprenorphine injection, synaptic facilitation was fully reversed. **C**, Spinal superfusion with DAAO (black bar, 1 U/ml) significantly reduced synaptic facilitation induced by ultra-low-dose buprenorphine (black arrow, dosing as in **A**). **D**, Spinal superfusion with the selective NMDAR antagonist D-AP5 (black bar, 100 μM) before bolus injection of ultra-low-dose buprenorphine (black arrow, dosing as in **A**) prevented facilitation of synaptic strength. For **A–D**, time courses of buprenorphine-treated animals are shown in black circles. Data are expressed as mean \pm SEM. Statistics: **A, B, D**, two-way ANOVA versus untreated controls (open circles) followed by Bonferroni *post hoc* test; **A**: $F_{(1,528)} = 18.52, p < 0.0001$; **B**: $F_{(1,127)} = 0.069, p = 0.79$; **D**: $F_{(1,549)} = 2.54, p = 0.111$; **C**, two-way ANOVA versus ultra-low-dose buprenorphine (open circles) followed by Bonferroni *post hoc* test; **C**: $F_{(1,725)} = 163.7, p < 0.0001$.

not induce OIH. One recent study reported that an ultra-low dose (0.1 $\mu\text{g}\cdot\text{kg}^{-1}$) of buprenorphine decreased tail-flick latencies in rats by an unknown mechanism (Wala and Holtman, 2011). Here, ultra-low-dose buprenorphine induced mechanical and thermal hyperalgesia in rats lasting for several hours after a single bolus injection. At doses that are one or two orders of magnitude higher than the dose used in the present study, buprenorphine facilitates a C-fiber-evoked motor reflex (Guirmand et al., 1995a; Guirmand et al., 1995b). Intrathecal injections of low-dose buprenorphine also facilitate action potential discharges of spinal dorsal horn convergent neurons (Dickenson et al., 1990). The present data extend these findings by showing that a single bolus injection of ultra-low-dose buprenorphine induced a slowly rising and long-lasting facilitation of synaptic strength at spinal C-fibers. Ultra-low-dose buprenorphine-induced facilitation was abolished in the presence of systemic naloxone hydrochloride or CTOP, but was affected by neither peripherally restricted nor spinally applied naloxone, nor by systemically applied naloxonazine. This suggests that ultra-low-dose buprenorphine-induced facilitation involves the activation of supraspinal naloxone-sensitive but naloxonazine-insensitive μ -opioid receptors.

In addition to activating μ -opioid receptors, opioids, including buprenorphine, have been shown to act on nonopioid receptors such as TLR4 in a naloxone-reversible manner (Hutchinson et al., 2010b). In the CNS, these receptors are predominantly expressed on glial cells (Olson and Miller, 2004; Jack et al., 2005) and their activation has been linked to opioid-induced tolerance and hyperalgesia (Watkins et al., 2009; Hutchinson et al., 2010a; Wang et al., 2012). Here, ultra-low-dose buprenorphine-induced facilitation was, however, abolished by intravenous application of the selective μ -opioid receptor antagonists CTOP and CTAP. In addition, we could show that ultra-low-dose buprenorphine-induced mechanical and thermal hyperalgesia was fully prevented in animals in which μ -opioid receptors were systemically blocked by CTOP. Although they do not rule out any additional effect of buprenorphine at TLR4s or other nonopioid receptors, our data clearly indicate that μ -opioid receptors are critically involved in ultra-low-dose buprenorphine-induced facilitation of synaptic strength.

Ultra-low-dose buprenorphine activates descending serotonergic pathways

Powerful descending pathways modulate discharges of spinal nociceptive neurons (Millan, 2002; Vanegas and Schaible, 2004; Heinricher et al., 2009; Sandkühler, 2009). Descending modulation has been associated with both, opioid-induced analgesia as well as OIH (Mitchell et al., 1998; Vanderah et al., 2001b; Gilbert and Franklin, 2002; Xie et al., 2005). Descending facilitation involves monoaminergic pathways. Here, surgical disruption of descending pathways and pharmacological blockade of spinal monoamine receptors by asenapine prevented ultra-low-dose buprenorphine-induced facilitation. Asenapine was effective when applied before or 15 min after buprenorphine injection, but not at a later time point. This suggests that monoamines that are released within the first minutes after an ultra-low-dose buprenorphine treatment are sufficient to trigger facilitation at spinal C-fiber synapses. The present data thus indicate that descending facilitatory pathways contribute to the induction of pain hypersensitivity and not just to its maintenance, as has been suggested previously (Burgess et al., 2002).

Descending pathways are the major source of serotonin in the spinal cord (Fields et al., 1991). In the spinal cord, the expression of 5-HT_{1,2,3,6,7}Rs has been demonstrated (Tecott et al., 1993; Helton et al., 1994; Gérard et al., 1996; Doly et al., 2005). Previously, we showed that morphine- and fentanyl-induced descending facilitation at C-fiber synapses requires the activation of spinal 5-HT₃Rs (Heinl et al., 2011). In contrast, blockade of spinal 5-HT₃Rs did not affect ultra-low-dose buprenorphine-induced facilitation in the present study. Serotonin also acts on spinal

5-HT_{2A}Rs, 5-HT_{2B}Rs, and 5-HT_{2C}Rs, which are coupled to phospholipase C and mobilize intracellular calcium (Barnes and Sharp, 1999). Agonists of the 5-HT_{2A}R and 5-HT_{2B}R subtypes potentiate transmission at spinal dorsal horn synapses (Hori et al., 1996; Aira et al., 2010; Rahman et al., 2011), and activation of these receptors may counteract opioid-induced depression of C-fiber-evoked field potentials (Aira et al., 2012). Topical application of 5-HT_{2A}R and 5-HT_{2B}R agonists TCB-2 and BW 723C86 induced long-lasting facilitation at spinal dorsal horn C-fiber synapses resembling ultra-low-dose buprenorphine-induced facilitation in terms of time course and level of potentiation (data not shown). Although activation of spinal 5-HT_{2A}Rs and 5-HT_{2B}Rs is apparently pronociceptive, the role of spinal 5-HT_{2C}Rs for nociception appears controversial. Their activation has been associated with anti-allodynia in neuropathic rats (Obata et al., 2001; Obata et al., 2004) and with the antinociceptive effects of serotonin in the formalin test (Jeong et al., 2004). Furthermore, 5-HT_{2C}R agonists can significantly depress C-fiber-evoked field potentials in both sham-operated and spinal-nerve-ligated animals (Aira et al., 2010). Conversely, systemic administration of mixed 5-HT_{2A/C} antagonists has been shown to inhibit C-fiber-evoked responses of deep dorsal horn neurons potently, suggesting pronociceptive effects of spinal HT_{2C}Rs (Rahman et al., 2011). Here, selective blockade of 5-HT_{2A}Rs, 5-HT_{2B}Rs, or 5-HT_{2C}Rs with their respective antagonists reduced and combined application abolished facilitation of synaptic strength induced by ultra-low-dose buprenorphine. Therefore, intrathecal application of all three 5-HT₂R antagonists also fully prevented ultra-low-dose buprenorphine-induced thermal and mechanical hyperalgesia, further supporting the pronociceptive potency of these receptor subtypes.

Spinal glial cells are required for ultra-low-dose buprenorphine-induced synaptic facilitation

5-HT₂Rs are expressed by neurons and astrocytes *in situ* and in culture (Hirst et al., 1998; Maxishima et al., 2001; Zhang et al., 2010). Here, activation of 5-HT_{2A}Rs, 5-HT_{2B}Rs, and 5-HT_{2C}Rs with selective agonists led to an increase in astrocytic calcium signaling in spinal cord slices that was significantly inhibited by the respective receptor antagonists. Emerging lines of evidence suggest that activation of spinal glial cells contribute to neuronal hyperexcitability after opioid exposure (Watkins et al., 2009; Ji et al., 2013). Here, blockade of spinal glial cells with the unspecific glial cell inhibitor fluorocitrate prevented ultra-low-dose buprenorphine-induced facilitation of synaptic strength. In addition, when fluorocitrate was applied to the spinal cord 2 h after ultra-low-dose buprenorphine, synaptic facilitation was fully reversed. Ultra-low-dose buprenorphine further led to an upregulation of the astrocytic marker GFAP (but not of the microglial marker Iba1) compared with vehicle-treated animals. This is consistent with a recent study suggesting that astrocytes but not microglia are activated upon administration of ultra-low-dose morphine (Sanna et al., 2015). These data suggest a role of spinal glial cells, putatively astrocytes, in both the initiation and maintenance of buprenorphine-induced descending facilitation. Activated astrocytes may release gliotransmitters that modulate synaptic transmission (Santello et al., 2012). For example, the gliotransmitter D-serine has been implicated in the development of morphine tolerance (Chen et al., 2012). In our experiments, degradation of D-serine by DAAO reduced ultra-low-dose buprenorphine-induced facilitation of C-fiber-evoked field potentials. D-serine acts as coagonist on NMDARs (Schell et al., 1995; Schell et al., 1997; Mothet et al., 2000), which have been linked previously to ultra-low-dose

buprenorphine-induced hyperalgesia (Wala and Holtman, 2011). Activation of spinal NMDARs was indeed required for ultra-low-dose buprenorphine-induced facilitation.

The present study revealed two opposite, dose-dependent effects of buprenorphine on synaptic transmission in the spinal dorsal horn. At analgesic doses, buprenorphine depressed synaptic transmission at C-fibers by the activation of spinal μ_1 -opioid receptors. However, a 15,000-fold lower dose of buprenorphine facilitated strength at spinal C-fiber synapses and induced the development of thermal and mechanical hyperalgesia. This implicates the activation of supraspinal CTOP-sensitive μ -opioid receptors and descending serotonergic pathways acting on spinal 5-HT_{2A}Rs, 5-HT_{2B}Rs, and 5-HT_{2C}Rs located on neurons, astrocytes, or both. D-serine, for example, that could be released from astrocytes after activation of astrocytic 5-HT_{2A}Rs, 5-HT_{2B}Rs, and 5-HT_{2C}Rs, might facilitate NMDAR activation and initiate a rise in $[Ca^{2+}]_i$, which culminates in an increase in synaptic strength.

References

- Aira Z, Buesa I, Salgueiro M, Bilbao J, Aguilera L, Zimmermann M, Azkue JJ (2010) Subtype-specific changes in 5-HT receptor-mediated modulation of C fibre-evoked spinal field potentials are triggered by peripheral nerve injury. *Neuroscience* 168:831–841. [CrossRef Medline](#)
- Aira Z, Buesa I, García del Caño G, Salgueiro M, Mendiola N, Mingo J, Aguilera L, Bilbao J, Azkue JJ (2012) Selective impairment of spinal μ -opioid receptor mechanism by plasticity of serotonergic facilitation mediated by 5-HT_{2A} and 5-HT_{2B} receptors. *Pain* 153:1418–1425. [CrossRef Medline](#)
- Angst MS, Clark JD (2006) Opioid-induced hyperalgesia: a qualitative systematic review. *Anesthesiology* 104:570–587. [CrossRef Medline](#)
- Barnes NM, Sharp T (1999) A review of central 5-HT receptors and their function. *Neuropharmacology* 38:1083–1152. [CrossRef Medline](#)
- Bryant RM, Olley JE, Tyers MB (1983) Antinociceptive actions of morphine and buprenorphine given intrathecally in the conscious rat. *Br J Pharmacol* 78:659–663. [CrossRef Medline](#)
- Burgess SE, Gardell LR, Ossipov MH, Malan TP Jr, Vanderah TW, Lai J, Porreca F (2002) Time-dependent descending facilitation from the rostral ventromedial medulla maintains, but does not initiate, neuropathic pain. *J Neurosci* 22:5129–5136. [Medline](#)
- Campbell ND, Lovell AM (2012) The history of the development of buprenorphine as an addiction therapeutic. *Ann N Y Acad Sci* 1248:124–139. [CrossRef Medline](#)
- Célèrier E, Laulin J, Larcher A, Le Moal M, Simonnet G (1999) Evidence for opiate-activated NMDA processes masking opiate analgesia in rats. *Brain Res* 847:18–25. [CrossRef Medline](#)
- Chaplan SR, Bach FW, Pogrel JW, Chung JM, Yaksh TL (1994) Quantitative assessment of tactile allodynia in the rat paw. *J Neurosci Methods* 53:55–63. [CrossRef Medline](#)
- Chen ML, Cao H, Chu YX, Cheng LZ, Liang LL, Zhang YQ, Zhao ZQ (2012) Role of P2X7 receptor-mediated IL-18/IL-18R signaling in morphine tolerance: multiple glial-neuronal dialogues in the rat spinal cord. *J Pain* 13:945–958. [CrossRef Medline](#)
- Christoph T, Kögel B, Schiene K, Méen M, De Vry J, Friderichs E (2005) Broad analgesic profile of buprenorphine in rodent models of acute and chronic pain. *Eur J Pharmacol* 507:87–98. [CrossRef Medline](#)
- Colpaert FC (1979) Can chronic pain be suppressed despite purported tolerance to narcotic analgesia? *Life Sci* 24:1201–1209. [CrossRef Medline](#)
- Cowan A, Lewis JW, Macfarlane IR (1977) Agonist and antagonist properties of buprenorphine, a new antinociceptive agent. *Br J Pharmacol* 60:537–545. [CrossRef Medline](#)
- Dickenson AH, Sullivan AF, McQuay HJ (1990) Intrathecal etorphine, fentanyl and buprenorphine on spinal nociceptive neurones in the rat. *Pain* 42:227–234. [CrossRef Medline](#)
- Dixon WJ (1965) The up-and-down method for small samples. *J Am Statist Assoc* 60:967–978. [CrossRef](#)
- Doly S, Fischer J, Brisorgueil MJ, Vergé D, Conrath M (2005) Pre- and postsynaptic localization of the 5-HT₇ receptor in rat dorsal spinal cord: Immunocytochemical evidence. *J Comp Neurol* 490:256–269. [CrossRef Medline](#)
- Drdla R, Gassner M, Gingl E, Sandkühler J (2009) Induction of synaptic

- long-term potentiation after opioid withdrawal. *Science* 325:207–210. [CrossRef Medline](#)
- Eidson LN, Murphy AZ (2013) Blockade of Toll-like receptor 4 attenuates morphine tolerance and facilitates the pain relieving properties of morphine. *J Neurosci* 33:15952–15963. [CrossRef Medline](#)
- Fields HL, Heinricher MM, Mason P (1991) Neurotransmitters in nociceptive modulatory circuits. *Annu Rev Neurosci* 14:219–245. [CrossRef Medline](#)
- Fukagawa H, Koyama T, Kakuyama M, Fukuda K (2013) Microglial activation involved in morphine tolerance is not mediated by toll-like receptor 4. *J Anesth* 27:93–97. [CrossRef Medline](#)
- Gardell LR, King T, Ossipov MH, Rice KC, Lai J, Vanderah TW, Porreca F (2006) Opioid receptor-mediated hyperalgesia and antinociceptive tolerance induced by sustained opiate delivery. *Neurosci Lett* 396:44–49. [CrossRef Medline](#)
- Gérard C, el Mestikawy S, Lebrand C, Adrien J, Ruat M, Traiffort E, Hamon M, Martres M-P (1996) Quantitative RT-PCR distribution of serotonin 5-HT₆ receptor mRNA in the central nervous system of control or 5,7-dihydroxytryptamine-treated rats. *Synapse* 23:164–173. [Medline](#)
- Gilbert AK, Franklin KB (2002) The role of descending fibers from the rostral ventromedial medulla in opioid analgesia in rats. *Eur J Pharmacol* 449:75–84. [CrossRef Medline](#)
- Guirimand F, Chauvin M, Willer JC, Le Bars D (1995a) Effects of intrathecal and intracerebroventricular buprenorphine on a C-fiber reflex in the rat. *J Pharmacol Exp Ther* 275:629–637. [Medline](#)
- Guirimand F, Chauvin M, Willer JC, Le Bars D (1995b) Effects of intravenous morphine and buprenorphine on a C-fiber reflex in the rat. *J Pharmacol Exp Ther* 273:830–841. [Medline](#)
- Hahn EF, Pasternak GW (1982) Naloxonazine, a potent, long-lasting inhibitor of opiate binding sites. *Life Sci* 31:1385–1388. [CrossRef Medline](#)
- Hahn EF, Carroll-Buatti M, Pasternak GW (1982) Irreversible opiate agonists and antagonists: the 14-hydroxydihydromorphinone azines. *J Neurosci* 2:572–576. [Medline](#)
- Hargreaves K, Dubner R, Brown F, Flores C, Joris J (1988) A new and sensitive method for measuring thermal nociception in cutaneous hyperalgesia. *Pain* 32:77–88. [CrossRef Medline](#)
- Heinke B, Gingl E, Sandkühler J (2011) Multiple targets of μ -opioid receptor mediated presynaptic inhibition at primary afferent A δ - and C-fibers. *J Neurosci* 31:1313–1322. [CrossRef Medline](#)
- Heinl C, Drdla-Schutting R, Xanthos DN, Sandkühler J (2011) Distinct mechanisms underlying pronociceptive effects of opioids. *J Neurosci* 31:16748–16756. [CrossRef Medline](#)
- Heinricher MM, Tavares I, Leith JL, Lumb BM (2009) Descending control of nociception: Specificity, recruitment and plasticity. *Brain Res Rev* 60:214–225. [CrossRef Medline](#)
- Helton LA, Thor KB, Baez M (1994) 5-hydroxytryptamine_{2A}, 5-hydroxytryptamine_{2B}, and 5-hydroxytryptamine_{2C} receptor mRNA expression in the spinal cord of rat, cat, monkey and human. *Neuroreport* 5:2617–2620. [CrossRef Medline](#)
- Hirst WD, Cheung NY, Rattray M, Price GW, Wilkin GP (1998) Cultured astrocytes express messenger RNA for multiple serotonin receptor subtypes, without functional coupling of 5-HT₁ receptor subtypes to adenylyl cyclase. *Brain Res Mol Brain Res* 61:90–99. [CrossRef Medline](#)
- Honsek SD, Walz C, Kafitz KW, Rose CR (2012) Astrocyte calcium signals at Schaffer collateral to CA1 pyramidal cell synapses correlate with the number of activated synapses but not with synaptic strength. *Hippocampus* 22:29–42. [CrossRef Medline](#)
- Hori Y, Endo K, Takahashi T (1996) Long-lasting synaptic facilitation induced by serotonin in superficial dorsal horn neurones of the rat spinal cord. *J Physiol* 492:867–876. [CrossRef Medline](#)
- Hoyer D, Clarke DE, Fozard JR, Hartig PR, Martin GR, Mylecharane EJ, Saxena PR, Humphrey PP (1994) International Union of Pharmacology classification of receptors for 5-hydroxytryptamine (serotonin). *Pharmacol Rev* 46:157–203. [Medline](#)
- Hutchinson MR, Zhang Y, Shridhar M, Evans JH, Buchanan MM, Zhao TX, Slivka PF, Coats BD, Rezvani N, Wieseler J, Hughes TS, Landgraf KE, Chan S, Fong S, Phipps S, Falke JJ, Leinwand LA, Maier SF, Yin H, Rice KC, et al. (2010b) Evidence that opioids may have toll-like receptor 4 and MD-2 effects. *Brain Behav Immun* 24:83–95. [CrossRef Medline](#)
- Hutchinson MR, Bland ST, Johnson KW, Rice KC, Maier SF, Watkins LR (2007) Opioid-induced glial activation: mechanisms of activation and implications for opioid analgesia, dependence, and reward. *ScientificWorldJournal* 7:98–111. [Medline](#)
- Hutchinson MR, Zhang Y, Brown K, Coats BD, Shridhar M, Sholar PW, Patel SJ, Crysdale NY, Harrison JA, Maier SF, Rice KC, Watkins LR (2008) Non-steroselective reversal of neuropathic pain by naloxone and naltrexone: involvement of toll-like receptor 4 (TLR4). *Eur J Neurosci* 28:20–29. [CrossRef Medline](#)
- Hutchinson MR, Lewis SS, Coats BD, Rezvani N, Zhang Y, Wieseler JL, Somogyi AA, Yin H, Maier SF, Rice KC, Watkins LR (2010a) Possible involvement of toll-like receptor 4/myeloid differentiation factor-2 activity of opioid inactive isomers causes spinal proinflammation and related behavioral consequences. *Neuroscience* 167:880–893. [CrossRef Medline](#)
- Ide S, Minami M, Satoh M, Uhl GR, Sora I, Ikeda K (2004) Buprenorphine antinociception is abolished, but naloxone-sensitive reward is retained, in μ -opioid receptor knockout mice. *Neuropsychopharmacology* 29:1656–1663. [CrossRef Medline](#)
- Ikeda H, Stark J, Fischer H, Wagner M, Drdla R, Jäger T, Sandkühler J (2006) Synaptic amplifier of inflammatory pain in the spinal dorsal horn. *Science* 312:1659–1662. [CrossRef Medline](#)
- Jack CS, Arbour N, Manusow J, Montgrain V, Blain M, McCreary E, Shapiro A, Antel JP (2005) TLR signaling tailors innate immune responses in human microglia and astrocytes. *J Immunol* 175:4320–4330. [CrossRef Medline](#)
- Jeong CY, Choi JI, Yoon MH (2004) Roles of serotonin receptor subtypes for the antinociception of 5-HT in the spinal cord of rats. *Eur J Pharmacol* 502:205–211. [CrossRef Medline](#)
- Ji RR, Berta T, Nedergaard M (2013) Glia and pain: Is chronic pain a gliopathy? *Pain* 154:S10–S28. [CrossRef Medline](#)
- Juni A, Klein G, Pintar JE, Kest B (2007) Nociception increases during opioid infusion in opioid receptor triple knock-out mice. *Neuroscience* 147:439–444. [CrossRef Medline](#)
- Kohno T, Kumamoto E, Higashi H, Shimoji K, Yoshimura M (1999) Actions of opioids on excitatory and inhibitory transmission in substantia gelatinosa of adult rat spinal cord. *J Physiol* 518:803–813. [CrossRef Medline](#)
- Lee M, Silverman SM, Hansen H, Patel VB, Manchikanti L (2011) A comprehensive review of opioid-induced hyperalgesia. *Pain Physician* 14:145–161. [Medline](#)
- Ling GS, Simantov R, Clark JA, Pasternak GW (1986) Naloxonazine actions in vivo. *Eur J Pharmacol* 129:33–38. [CrossRef Medline](#)
- Lutfy K, Cowan A (2004) Buprenorphine: a unique drug with complex pharmacology. *Curr Neuropharmacol* 2:395–402. [CrossRef Medline](#)
- Lutfy K, Eitan S, Bryant CD, Yang YC, Salimnejad N, Walwyn W, Kieffer BL, Takeshima H, Carroll FI, Maidment NT, Evans CJ (2003) Buprenorphine-induced antinociception is mediated by μ -opioid receptors and compromised by concomitant activation of opioid receptor-like receptors. *J Neurosci* 23:10331–10337. [Medline](#)
- Mao J, Price DD, Mayer DJ (1995) Mechanisms of hyperalgesia and morphine tolerance: a current view of their possible interactions. *Pain* 62:259–274. [CrossRef Medline](#)
- Mattioli TA, Leduc-Pessah H, Skelhorne-Gross G, Nicol CJ, Milne B, Trang T, Cahill CM (2014) Toll-like receptor 4 mutant and null mice retain morphine-induced tolerance, hyperalgesia, and physical dependence. *PLoS One* 9:e97361. [CrossRef Medline](#)
- Maxishima M, Shiga T, Shutoh F, Hamada S, Maeshima T, Okado N (2001) Serotonin 2A receptor-like immunoreactivity is detected in astrocytes but not in oligodendrocytes of rat spinal cord. *Brain Res* 889:270–273. [CrossRef Medline](#)
- Mestre C, Pélissier T, Fialip J, Wilcox G, Eschalié A (1994) A method to perform direct transcutaneous intrathecal injection in rats. *J Pharmacol Toxicol Methods* 32:197–200. [CrossRef Medline](#)
- Millan MJ (2002) Descending control of pain. *Prog Neurobiol* 66:355–474. [CrossRef Medline](#)
- Mitchell JM, Lowe D, Fields HL (1998) The contribution of the rostral ventromedial medulla to the antinociceptive effects of systemic morphine in restrained and unrestrained rats. *Neuroscience* 87:123–133. [CrossRef Medline](#)
- Mothet -P, Parent AT, Wolosker H, Brady RO Jr, Linden DJ, Ferris CD, Rogawski MA, Snyder SH (2000) D-serine is an endogenous ligand for the glycine site of the N-methyl-D-aspartate receptor. *Proc Natl Acad Sci U S A* 97:4926–4931. [CrossRef Medline](#)
- Obata H, Saito S, Sasaki M, Ishizaki K, Goto F (2001) Antiallostatic effect of

- intrathecally administered 5-HT₂ agonists in rats with nerve ligation. *Pain* 90:173–179. [CrossRef Medline](#)
- Obata H, Saito S, Sakurazawa S, Sasaki M, Usui T, Goto F (2004) Antiallo-dynamic effects of intrathecally administered 5-HT_{2C} receptor agonists in rats with nerve injury. *Pain* 108:163–169. [CrossRef Medline](#)
- Olson JK, Miller SD (2004) Microglia initiate central nervous system innate and adaptive immune responses through multiple TLRs. *J Immunol* 173:3916–3924. [CrossRef Medline](#)
- Ossipov MH, Lai J, King T, Vanderah TW, Malan TP Jr, Hruby VJ, Porreca F (2004) Antinociceptive and nociceptive actions of opioids. *J Neurobiol* 61:126–148. [CrossRef Medline](#)
- Pasternak GW, Pan -X (2013) Mu opioids and their receptors: evolution of a concept. *Pharmacol Rev* 65:1257–1317. [CrossRef Medline](#)
- Pert CB, Snyder SH (1973) Opiate receptor: demonstration in nervous tissue. *Science* 179:1011–1014. [CrossRef Medline](#)
- Rahman W, Bannister K, Bee LA, Dickenson AH (2011) A pronociceptive role for the 5-HT₂ receptor on spinal nociceptive transmission: an in vivo electrophysiological study in the rat. *Brain Res* 1382:29–36. [CrossRef Medline](#)
- Sandkühler J (2009) Models and mechanisms of hyperalgesia and allodynia. *Physiol Rev* 89:707–758. [CrossRef Medline](#)
- Sanna MD, Ghelardini C, Galeotti N (2015) Activation of JNK pathway in spinal astrocytes contributes to acute ultra-low dose morphine thermal hyperalgesia. *Pain*.
- Santello M, Cali C, Bezzi P (2012) Gliotransmission and the tripartite synapse. *Adv Exp Med Biol* 970:307–331. [CrossRef Medline](#)
- Schell MJ, Molliver ME, Snyder SH (1995) D-serine, an endogenous synaptic modulator: localization to astrocytes and glutamate-stimulated release. *Proc Natl Acad Sci U S A* 92:3948–3952. [CrossRef Medline](#)
- Schell MJ, Brady RO Jr, Molliver ME, Snyder SH (1997) D-serine as a neuromodulator: regional and developmental localizations in rat brain glia resemble NMDA receptors. *J Neurosci* 17:1604–1615. [Medline](#)
- Shahid M, Walker GB, Zorn SH, Wong EH (2009) Asenapine: a novel psychopharmacologic agent with a unique human receptor signature. *J Psychopharmacol* 23:65–73. [CrossRef Medline](#)
- Simonnet G, Rivat C (2003) Opioid-induced hyperalgesia: abnormal or normal pain? *Neuroreport* 14:1–7. [CrossRef Medline](#)
- Suzuki R, Rygh LJ, Dickenson AH (2004) Bad news from the brain: descending 5-HT pathways that control spinal pain processing. *Trends Pharmacol Sci* 25:613–617. [CrossRef Medline](#)
- Tecott LH, Maricq AV, Julius D (1993) Nervous system distribution of the serotonin 5-HT₃ receptor mRNA. *Proc Natl Acad Sci U S A* 90:1430–1434. [CrossRef Medline](#)
- Van Dorpe S, Adriaens A, Polis I, Peremans K, Van Bocxlaer J, De Spiegeleer B (2010) Analytical characterization and comparison of the blood-brain barrier permeability of eight opioid peptides. *Peptides* 31:1390–1399. [CrossRef Medline](#)
- Vanderah TW, Ossipov MH, Lai J, Malan TP Jr, Porreca F (2001a) Mechanisms of opioid-induced pain and antinociceptive tolerance: descending facilitation and spinal dynorphin. *Pain* 92:5–9. [CrossRef Medline](#)
- Vanderah TW, Suenaga NM, Ossipov MH, Malan TP Jr, Lai J, Porreca F (2001b) Tonic descending facilitation from the rostral ventromedial medulla mediates opioid-induced abnormal pain and antinociceptive tolerance. *J Neurosci* 21:279–286. [Medline](#)
- Vanegas H, Schaible HG (2004) Descending control of persistent pain: inhibitory or facilitatory? *Brain Res Brain Res Rev* 46:295–309. [CrossRef Medline](#)
- Wala EP, Holtman JR Jr (2011) Buprenorphine-induced hyperalgesia in the rat. *Eur J Pharmacol* 651:89–95. [CrossRef Medline](#)
- Wang X, Loram LC, Ramos K, de Jesus AJ, Thomas J, Cheng K, Reddy A, Somogyi AA, Hutchinson MR, Watkins LR, Yin H (2012) Morphine activates neuroinflammation in a manner parallel to endotoxin. *Proc Natl Acad Sci U S A* 109:6325–6330. [CrossRef Medline](#)
- Watkins LR, Hutchinson MR, Rice KC, Maier SF (2009) The “toll” of opioid-induced glial activation: improving the clinical efficacy of opioids by targeting glia. *Trends Pharmacol Sci* 30:581–591. [CrossRef Medline](#)
- Waxman AR, Arout C, Caldwell M, Dahan A, Kest B (2009) Acute and chronic fentanyl administration causes hyperalgesia independently of opioid receptor activity in mice. *Neurosci Lett* 462:68–72. [CrossRef Medline](#)
- Wolozin BL, Pasternak GW (1981) Classification of multiple morphine and enkephalin binding sites in the central nervous system. *Proc Natl Acad Sci U S A* 78:6181–6185. [CrossRef Medline](#)
- Xie JY, Herman DS, Stiller CO, Gardell LR, Ossipov MH, Lai J, Porreca F, Vanderah TW (2005) Cholecystokinin in the rostral ventromedial medulla mediates opioid-induced hyperalgesia and antinociceptive tolerance. *J Neurosci* 25:409–416. [CrossRef Medline](#)
- Xu JT, Zhao JY, Zhao X, Ligons D, Tiwari V, Atianjoh FE, Lee CY, Liang L, Zang W, Njoku D, Raja SN, Yaster M, Tao YX (2014) Opioid receptor-triggered spinal mTORC1 activation contributes to morphine tolerance and hyperalgesia. *J Clin Invest* 124:592–603. [CrossRef Medline](#)
- Yamamoto T, Shono K, Tanabe S (2006) Buprenorphine activates μ and opioid receptor like-1 receptors simultaneously, but the analgesic effect is mainly mediated by μ -receptor activation in the rat formalin test. *J Pharmacol Exp Ther* 318:206–213. [CrossRef Medline](#)
- Zhang S, Li B, Lovatt D, Xu J, Song D, Goldman SA, Nedergaard M, Hertz L, Peng L (2010) 5-HT_{2B} receptors are expressed on astrocytes from brain and in culture and are a chronic target for all five conventional ‘serotonin-specific reuptake inhibitors’. *Neuron Glia Biol* 6:113–125. [CrossRef Medline](#)